Elsevier Editorial System(tm) for Cement and Concrete Composites

Manuscript Draft

Manuscript Number:

Title: Autogenous healing on the recovery of mechanical performance of High Performance Fibre Reinforced Cementitious Composites (HPFRCCs): part 2 - correlation between healing of mechanical performance and crack sealing

Article Type: Research Paper

Keywords: self healing, high performance fibre reinforced cementitious composites, crack sealing, healing indices

Corresponding Author: Prof. Liberato Ferrara, PhD

Corresponding Author's Institution: Politecnico di Milano

First Author: Liberato Ferrara, PhD

Order of Authors: Liberato Ferrara, PhD; Visar Krelani, PhD; Fabio Moretti, MSc Eng

Abstract: This paper is the second part of a companion paper study focused on the autogenous self-healing capacity of High Performance Fibre Reinforced Cementitious Composites (HPFRCCs). In part 1 the capacity of the material has been investigated to completely or partially re-seal the cracks, as a function of its composition, maximum crack width and exposure conditions. Different flow induced alignment of fibres, with respect to the applied bending stresses have been also considered. The outcomes of the self-healing phenomenon, have been analysed in terms of recovery of stiffness, strength and ductility, as measured by means of 4-point bending tests, performed before (pre-cracking) and after the conditioning exposure. In a durability-based design framework, self-healing indices quantifying the recovery of mechanical properties were also defined and their significance cross-checked. In this paper the crack closure will be evaluated, both through visual image analysis of the healed cracks as well as through a tailored indirect method, proposed by the first authors in a previous study. This method is based on the comparative analysis of the damage evolution curves built for both the pre-cracked and the healed stages from the evaluation of the flexural stiffness. Recovery of mechanical properties will hence be correlated to the identified amount of crack closure. In the authors' opinion, this step represents a fundamental contribution in order to reliably and consistently incorporate the effects of self-healing into tailored durability-based design approaches, based, e.g., on a "healable" crack width threshold concept.

**Cover Letter**

Milan, December 23, 2015

To the Editor in Chief of

Cement and Concrete Composites

**Subject:** submission of manuscript for review and publication in CCC

Dear Editor in Chief

Please find attached the manuscript of the paper

**Autogenous healing on the recovery of mechanical performance of High Performance Fibre Reinforced Cementitious Composites (HPFRCCs): part 2 – correlation between healing of mechanical performance and crack sealing**

Authored by myself, dr. Visar Krelani, Fabio Moretti.

This manuscript has to be intended as a companion paper submission with manuscript

**Effects of autogenous healing on the recovery of mechanical performance of High Performance Fibre Reinforced Cementitious Composites (HPFRCCs): part 1**

Authored by myself, dr. Visar Krelani, Fabio Moretti, Marta Roig FLores and prof. Pedro Serna (submitted for publication to CCC – manuscript CCC-S-15-00998).

Thank you for your consideration

ALso on behalf of my coatuhors

Yours sincerely

Liberato Ferrara

PhD, associate professor

# Autogenous healing on the recovery of mechanical performance of High Performance Fibre Reinforced Cementitious Composites (HPFRCCs): part 2 – correlation between healing of mechanical performance and crack sealing

*Liberato Ferrara*[1,2], *Visar Krelani*[1,3] *and Fabio Moretti*[1],

## ABSTRACT



This paper is the second part of a companion paper study focused on the autogenous self-healing capacity of High Performance Fibre Reinforced Cementitious Composites (HPFRCCs). In part 1 the capacity of the material has been investigated to completely or partially re-seal the cracks, as a function of its composition, maximum crack width and exposure conditions. Different flow induced alignment of fibres, with respect to the applied bending stresses have been also considered. The outcomes of the self-healing phenomenon, have been analysed in terms of recovery of stiffness, strength and ductility, as measured by means of 4-point bending tests, performed before (pre-cracking) and after the conditioning exposure. In a durability-based design framework, self-healing indices quantifying the recovery of mechanical properties were also defined and their significance cross-checked. In this paper the crack closure will be evaluated, both through visual image analysis of the healed cracks as well as through a tailored indirect method, proposed by the first authors in a previous study. This method is based on the comparative analysis of the damage evolution curves built for both the pre-cracked and the healed stages from the evaluation of the flexural stiffness. Recovery of mechanical properties will hence be correlated to the identified amount of crack closure. In the authors' opinion, this step represents a fundamental contribution in order to reliably and consistently incorporate the effects of self-healing into tailored durability-based design approaches, based, e.g., on a "healable" crack width threshold concept.

[1] Department of Civil and Environmental Engineering, Politecnico di Milano, piazza Leonardo da Vinci 32, 20133 Milano, Italy.
[2] Corresponding author, email: liberato.ferrara@polimi.it
[3] now at University for Business and Technology, Kalabria, Prishtinë 10000, Kosova.

## 1. Introduction

Self-healing cement based materials are a valuable asset for the XXI century civil engineering, able to provide a technically effective and economically competitive solution to the increasingly urging problem of deteriorating and hence repair-needing building structures and infrastructure facilities.

The huge amount of research data produced in the last decade [1,2] have made it possible the realization of the earliest demonstrative prototypes (the self-healing concrete pavilion in Breda, The Netherlands, [3]). but also a few pioneer full scale applications. Among these the following are worth citing: an irrigation canal built in Ecuador (a synergy between TU Delft and Universidade Catolica de Santiago de Guayaquil, [4]) with self-healing concrete containing bacteria; the underground/underwater structures of the Changi airport in Singapore where the use of crystalline admixtures, originally meant as porosity reducers for waterproofing also resulted into an effective crack sealing activity [5]; and a highway strip in the Netherlands A58 made with self-healing porous asphalt [6, 7].

Evidence of the ability of the different aforementioned self-healing techniques to seal the cracks, depending on their width, exposure conditions etc. has been widely proved in the laboratory. In very recent years interest and concern has also arisen in the engineering community about the efficacy of these techniques not only to seal the cracks and restore material imperviousness to the ingress of water and other aggressive harmful substances but also to “heal” the material. This refers to the ability of providing a (partial) recovery of the pristine level of engineering and mechanical performance, in terms of, e.g., load and deformation capacity, stiffness etc., which are evidently impaired by cracks and damages.

As a matter of fact such a capacity of healing the material properties will depend not merely on the amount of crack healing but also on the nature of the healing products, and hence on the healing mechanisms, whether driven by delayed hydration producing stronger CSH crystals or by carbonation resulting into weaker $CaCO_3$ crystals, by the age of the healing products and of the substrate which also affects the degree of reciprocal compatibility and hence the effectiveness of the

"through crack" material continuity restoration.

The interest vs. the recovery of material mechanical performance has increased with the advent and spread in the construction market of Fibre Reinforced Concrete (FRC) and Cementitious Composites (FRCCs). These materials exhibit a not negligible post-cracking residual strength, in some cases even featuring a strain hardening tensile behaviour. These tensile strength and toughness parameters do explicitly enter into design approaches for FRC structures [8]. In view of the aforementioned concept, the capacity of the material to regain a higher post-cracking residual strength or retaining its target design value for a longer time rightly due to crack healing phenomena may represent an added value not only in terms of better and longer durability but also in terms of a longer lasting structural performance, which may result into delayed first repair time, and into an overall lower life cycle cost.



An attempt to correlate the amount of recovery of load bearing capacity and stiffness of ordinary concrete to the amount of crack sealing has been made by Ferrara et al. [9], who showed that the strength recovery is lower than stiffness one and that anyway a crack-sealing threshold (e.g. 50 to 60% of its initial amount) has to be overcome to start appreciating some recovery of the mechanical performance. Qualitatively and quantitatively similar results have been obtained by Roig Flores et al. [10] with reference to the correlation between recovery of water flow tightness and crack sealing.

In a previous comparative study [11], Ferrara et al. have provided an extensive investigation on the ability of High Performance Fibre Reinforced Cementitious Composites (HPFRCCs) to recover, thanks to autogenous healing, their mechanical performance in terms of stiffness, strength and deformation capacity even for quite high values of initial crack openings (up to 0.5 mm) and for quite old first cracking age (about one year). The peculiar composition of the aforementioned category of cement based materials, featuring high cement and binder content and low w/b ratios, makes them highly conducive to feature an autogenous healing capacity, obviously as a function of the exposure conditions and duration and initial cracking stage. Cracks in fact expose clusters of un-

hydrated binder particles to air moisture and, in case, water, which can thus not only activate delayed hydration reactions but also promote leaching of calcium hydroxide from the matrix to form calcium carbonate crystals with the carbon dioxide dissolved in the same water.

The recovery of the mechanical performance has been quantified by means of a tailored experimental methodology, consisting in pre-cracking the specimens in four point bending, conditioning them in different environments and for different durations (up to two years), and then re-testing them up to failure according to the same set-up employed for pre-cracking. Comparative analysis of the stress vs. crack opening curves recorded in the pre-cracking and post-conditioning tests for each and all the specimens stand as the key process step to assess the effectiveness of healing on the recovery of the mechanical performance.

In this paper the amount of recovery of mechanical performance, in terms of strength, deformation capacity (ductility) and stiffness will be correlated, as a function of the experimental variables defined above, to the amount of crack closure. This has been directly measured and quantified from image analysis processing of crack processing, garnered after pre-cracking and after post-conditioning, and also indirectly estimated by means of a tailored method [9] based on the comparison between either pre-cracking/post-conditioning damage vs. crack opening evolution curves. These have been built through a best fitting of the stiffness decay and recovery, as measured through instantaneous loading/unloading cycles performed all along both pre-cracking and post-conditioning tests. The availability of different crack healing measures as above will allow to assess their reliability. Moreover, the correlation between indices of recovery of different mechanical properties and different indices of crack sealing will also be instrumental at having a deeper insight into the effectiveness of healing mechanisms and their effects. This represents an absolute novelty, to the authors' knowledge, in the literature on the topic and is a much needed step for the coherent incorporation of self-healing concepts into crack-opening based durability limit states design approaches for structures, either built of or retrofitted with fibre reinforced cementitious composites.

## 2. Indices of recovery of mechanical properties

In a previous companion study an extensive survey about the self-healing capacity of a HPFRCC (detailed mix composition in Table 1) has been performed employing dedicated experimental methodology [11], as explained in the introductory section. Through the comparison of nominal bending stress vs. Crack Opening curves obtained from 4-point bending tests performed on the same specimens in a pre-cracking and post-conditioning regime (Figure 1) the effect of crack sealing, if any, on the recovery of mechanical performance of the material has been evaluated. Since the influence of the flow-induced orientation of fibres on the deflection behaviour (whether strain softening or hardening) was explicitly introduced as an experimental variable in the programme, the pre-crack opening was different for different deflection behaviours, as it can be also observed in Table 2 where a synopsis of the programme is reported.



Recovery of mechanical properties was also evaluated in different ways depending on the deflection hardening or softening behaviour, as well as on the pre-crack opening, as already detailed in [8] and as hereafter summarized for the sake of paper readability.

- *Stress recovery:* In the case of deflection softening specimens as well as of deflection hardening specimens pre-cracked up to $COD_{peak}$ + 0.5 mm, the recovery of load/stress bearing capacity promoted by the crack healing can be effectively evaluated as illustrated in Figures 2a-b.

  For deflection hardening specimens pre-cracked in the pre-peak regime (i.e. up to 1mm and 2 mm), the definition of the index of stress recovery has to be cleansed of the increase of load bearing capacity that the specimen would have inherently shown to reach the peak due to its deflection hardening behaviour associated to stable multiple cracking (Figure 2c).

  It is furthermore worth remarking that, as from the experimental procedure detailed in the companion paper [8] the measured Crack Opening Displacement (COD) in the case of deflection softening specimens represents the opening of the single localized crack. On the other hand, for deflection hardening specimens, it is an integral of all the multiple cracks which form along the pre-peak stable multiple cracking stage in the central, constant bending moment,

region of the specimen. As a matter of fact, since the spacing of the cracks resulted close to the fibre length, about 12 cracks formed in the region above, which can be reasonably hypothesized to be uniformly opened.

A further distinction has to be made in the case of deflection hardening specimens pre-cracked up to $COD_{peak}$ +0 .5 mm: the further post-peak crack opening (0.5 mm) has to be attributed uniquely to the major crack which unstably localizes after the peak, whereas up to the peak the crack opening ($COD_{peak}$) is uniformly distributed among all the multiple cracks as above.



- *Stiffness recovery:* it has been computed as the difference between the tangent reloading stiffness in the post-conditioning test and the secant unloading stiffness in the pre-cracking one, divided by the loss of stiffness which occurred during the same pre-cracking test (Figure 3).
- *Ductility recovery: f*or deflection hardening specimens the effects of crack healing on the recovery of ductility have been also evaluated, with reference to both peak and post-peak regime. For specimens pre-cracked in the pre-peak regime, as graphically explained in Figure 4a/5a, healing can be deemed to occur if and only if the ductility measured in the post-conditioning test exceeds the one that the specimen in its virgin state would have anyway exhibited. On the other hand specimens pre-cracked up to $COD_{peak}$ + 0.5 mm (Figure 4b/5b) would be considered healed if able to exhibit, in the reloading post conditioning test is a ductility, measured as the crack opening at the post-conditioning peak minus the pre-crack opening, at least equal to the one exhibited in the pre-cracking test.

Table 3 reports a summary of numerical values of all the Healing Indices calculated as above.

In the cited companion paper study [11] these have been extensively discussed, with reference to the influence of exposure conditions and durations, as well as of the initial crack opening, yielding to the following main statements:

- the healing results in terms of load bearing capacity and stiffness show an improvement of these properties, continuously growing with ongoing exposure even if to a different extent as a function of the exposure conditions.

- in general, presence of water, even in form of high air humidity or in the case of wet and dry cycles, favoured faster and higher healing. Moreover, prolonged exposure, even after two years, continued to induce healing, even if in some cases at a lower rate than in the early exposure times.
- on the other hand, in terms of ductility, the recovery features a worsening trend with time of exposure. This can be explained by taking into account that self-healing products, restoring the material "cross-crack" continuity and hence its "through-crack" load bearing capacity, also negatively affect, e.g. through some local bond increase, the transfer length and the consequent stress redistribution capacity which is responsible of ductility. As a matter of fact, upon post-conditioning tests, reopening of the previously formed cracks was always observed, and in no case a new crack formed at another location.



In the following, indices of recovery of mechanical properties, as above, will be correlated to the amount of crack sealing, evaluated through image analysis processing of visually observed cracks (optical microscopy) as well as through an indirect procedure based on the comparison between post-conditioning and pre-cracking damage evolution curves [6]. Both procedures are going to be detailed hereafter.

## 3. Crack opening measurements and crack sealing evaluation

### *3.1 Image analysis processing of cracks observed by optical microscopy*

The measurement of crack geometrical parameters (width and area) is based on the study of pictures showing the cracks all along their length, as obtained by means of digital optical microscope before and after the healing exposure at different magnifications (x50, x 200). The photography software Adobe Photoshop CS6 was used for image processing.

An example of the crack pattern surveying procedure for both deflection softening and hardening specimens is shown in Figure 6. It is worth remarking that for deflection softening specimens and

deflection hardening specimens pre-cracked in the post-peak regime only one crack had to be measured, which is the single crack or the crack unstably localizing after the peak respectively. On the other hand, for deflection hardening specimens pre-cracked in the pre-peak regime all multiple formed cracks were monitored and the measures have been then averaged.

This method is more precise and reliable than the measurements which can be obtained by using the transparent calibration ruler since through the use of the graphical software is possible to choose the real width bypassing the error related to the human eye, which in small cracks, as those studied in this research, becomes more relevant.



Three different measures were taken:

- *Measure of crack width:*

  $w_{max}$, *maximum crack width:* by means of graphic software, the maximum crack width is determined in millimetres (Figure 7a);

  $w_{avg}$, *average crack width:* by means of graphic software, crack width (in millimeters) is determined at three fixed positions (approximately located 10 mm from the edges of the pictograph and at mid-length of the surveyed portion of the crack) and averaged (Figure 7b);

- *Measure of crack area:*

  $A_{px}$, *measuring black pixels:* by using graphic software, black pixels in the image are counted, which indicate crack area (Figure 7c). The calculation of the crack area involved the use of the graphical software to quantify the number of black pixels inside the pictures. The basic concept is that the cracks are shown as a black area, thus a higher number of black pixels correspond to a greater area of the crack. In order to avoid that pores or other dark parts of the pictures that may affect the quantification of black pixels, all the panoramas pictures have were been cleaned by a specific tool of the software.

### *3.2 Crack closure estimate from damage evolution curves*

As shown by the sample nominal stress $\sigma_N$ vs. COD curve in Figure 8, all along the 4pb test loading

path, both in the pre-cracking and post-conditioning stages, a series of "instantaneous" unloading-reloading cycles was performed. This allowed the values of secant unloading stiffness, $K_{U,j}$, to be evaluated in correspondence of different values of the Crack Opening Displacement, CODj, through which corresponding values could be calculated of a Continuum Damage variable, coherently meant as an index of stiffness degradation:

$$D(CODj) = 1 - \frac{K_{U,j}}{K_{L,1}} \quad (1)$$



where $K_{L,1}$ is the tangent loading stiffness upon the first loading branch, coherently with notation once again explained in Figure 7. It was thus possible to build up the evolution laws of the damage variable vs. COD, through an exponential fitting of the data as:

$$D(COD) = \exp[-A/COD] \quad (2)$$

where A is a fitting constant, correlated to the speed of damage accumulation with progressive crack opening: the higher A, the slower the damage growth. Damage evolution laws built as above are shown in Figures 9 for all the tested specimens.

The effects of self-healing, as affected by the different exposure conditions and durations as well as of the pre-crack openings, can be clearly got from the "slowering" trends of the damage evolution laws, as built with reference to the results of pre-cracking tests on virgin specimens or to the post-conditioning failure tests performed on healed specimens.

In order to estimate crack closure from damage evolution curves the following methodology proposed by Ferrara et al. [9] has been employed. It consists first of all (Figure 10) in identifying the points representative of damage-COD, as evaluated upon reloading the specimen after environmental conditioning, assuming the initial crack opening coincided with the value measured at unloading during the pre-cracking stage. The points, identified as above, are then "shifted backward" along the COD axis until the fitted damage-COD evolution curve of the virgin specimen is met: the amount of this backward shifting can be assumed as an indicator of the crack closure effect produced by the self-healing phenomena.

### *3.3 Index of crack healing*

From the values of crack-opening, measured and/or estimated both in the pre-cracking and in the post-conditioning regime an Index of Crack Healing has been defined as follows:

$$\text{Index of Crack Healing ICH} = 1 - \frac{\text{COD}_{\text{post-conditioning}}}{\text{COD}_{\text{pre-cracking}}} \quad (3)$$

As for the visually evaluated crack parameters a correlation between the indices calculated from different measurements is shown in Figure 11 a-b, highlighting the coherence of the garnered measurements and of the calculated indices. Also in accordance with the outcomes of a previous study [10] the index based on the measurement of an average crack opening was henceforth employed.



The Indices of Crack Healing calculated from visual crack processing as well as from the indirect procedure based on the comparison of damage evolution curves are respectively shown in Figures 12 a-d and 13 a-d and furthermore compared to each other in Figure 14.

It is interesting to observe that, whereas the Index of Crack Healing evaluated from image processing spans all over the available data range (0-1), in the case of the index evaluated from damage recovery, data are concentrated in a narrower range. This evidently results in the fact that also specimens characterized by a lower visual crack healing are likely to have experience a moderately significant crack closure as indirectly evaluated through the recovery of stiffness.

This discrepancy can be explained by considering that the “sealing/healing” of the crack reasonably starts from its tip and hence even in specimens which do not feature evident closure of the cracks at their surface, some precipitation of self-healing products may have occurred in the inner parts of the cracks [10] thus leading to some recovery of stiffness. Moreover, the same fitting procedure employed to build the damage evolution curves from computed stiffness decaying may have led to some overestimation of the related estimate of crack closure, mainly in the case of smaller healing.

Anyway, the whole corpus of the results provides a further confirmation to the statements exposed above with reference to the indices of recovery of mechanical properties. The coherence of the

whole set of results garnered so far through the definition of different self-healing indices, may also stand as a proof of the reliability of the proposed methodology for the evaluation of effects of self healing on the recovery of mechanical performance of HPFRCCs.

### *3.4 Comparison Indices of Mechanical Properties Recovery and Index of Crack Healing*



The different indices of recovery of material and specimen/structural mechanical properties have been finally compared with the Index of Crack Healing, evaluated through both methodologies exposed above. The results are shown in Figures 15 a-b to 18 a-b.

The sparsity of the results, processed as a whole, should not be deceptive about the reliability and significance of this analysis, since it is evidently due to the wide set of experimental variables which have been considered in this investigation (deflection hardening/softening behavior, crack-opening, exposure conditions and durations). The analysis yields clearer outputs if the five herein considered exposure conditions are separately dealt with.

It can be first of all observed that the identified correlation trends are substantially similar, no matter whether the Index of Crack Healing has been evaluated from image processing of crack pictures or from the damage evolution curves. This clearly supports the reliability of both indices as well as of their calculation procedure.

With reference to both the evolution of the strength and stiffness recovery with crack closure, it can be clearly observed that a significant crack healing (greater than, e.g., 60 to 80%) is necessary before any recovery of the either mechanical properties can be appreciated. Influence os exposure conditions is as expected, and as analyzed in detail in [8], with reference to both the amount of recovery and to the scattering of the results, and hence to the neatness of the inferred trends.

Significantly, the Index of Ductility Recovery, both in the pre- and post-peak regimes, shows a higher scattered and somewhat decreasing trend with respect to the increase of crack closure. As already explained in detail in [11], the self-healing products, restoring the material “cross-crack” continuity and hence its “through-crack” load bearing capacity, also negatively affect, e.g. through

some local bond increase, the transfer length and the consequent stress redistribution capacity which is responsible of ductility.

Visual confirmation of the healed cracks and correlation with the different calculated indices of recovery of mechanical properties and of crack closure can be clearly appreciated from sample pictures shown in Figure 19 a-c to 21 a-c.



## 4. Conclusions

This paper reports the second part of a thorough experimental investigation on the self-healing capacity of High Performance Fibre Reinforced Cementitious (HPFRCCs). This is mainly due to the peculiar mix composition of this signature category of advanced cement based materials, featuring high binder content and low water/binder ratios, which is likely to leave, in the bulk of a specimen/structural element, significant amount of un-hydrated binder particles. These, upon cracking, may come in contact with water and/or atmosphere humidity, thus undergoing delayed hydration reactions whose products precipitate onto the crack surfaces and seal them also allowing, thanks to restored through-crack material continuity, to regain to some extent the pristine level of mechanical performance.

In first part of the study [11], the recovery of different mechanical properties, including stiffness, load-bearing and deformation capacity, as measured by means of 4-point bending tests performed before and after the healing period, has been evaluated as a function of the exposure conditions (ranging from water immersion to wet and dry cycles, to exposure to natural environment or conditioned wet or dry air) and durations (up to two years). In this paper, the effects of crack healing on the recovery of mechanical properties have been correlated to the amount of crack closure, quantified by means of two tailored “direct” and “indirect” procedures.

The former is bases on image analysis of pictures of crack patterns, acquired both after the initial damage was induced in the specimens and at the end of the healing/conditioning period.

The latter, on its hand, is based on the comparative analysis of damage vs. crack opening evolution

curves, built through a dedicated procedure from experimental 4-point bending test results.

The results have clearly shown that a significant crack closure (greater than 60 to 80%) is necessary before any significant recovery in terms of strength and stiffness could be appreciated. Influence of exposure conditions was as expected, in the sense that the higher availability of water resulted in better and less scattered recovery of mechanical performance. Moreover, quite interestingly, the recovery of mechanical performance continued even after quite longer exposure times, obviously up to complete closure of the cracks, from which point on a steady recovery response was observed. This cast high interest on the possibility of exploiting the outcomes of self-healing in true engineering applications, where the effectiveness of healing cannot and must not be limited to usual (short) laboratory-investigation times.



On the other hand it was observed that the ductility of the material/specimens featured some recovery but decreasing with the amount of crack sealing. As explained above, this may be reasonably explained by hypothesizing that the self-healing products, restoring the material "cross-crack" continuity and hence its "through-crack" load bearing capacity, also negatively affect, e.g. through some local bond increase, the transfer length and the consequent stress redistribution capacity which is responsible of ductility.

The quite solid correlation established between suitably defined indices quantifying the recovery of mechanical properties and the amount of crack healing confirms the reliability of the experimental procedure herein proposed and employed to assess the self-healing capacity of HPFRCCs. This may result, in order to incorporate the effects of crack healing into a durability-based design framework, into the implementation of a "healable crack width", defined as a function of the material composition and of the anticipated/expected exposure and service conditions, replacing the fixed "allowable crack width" concept as currently formulated in the design codes.

In order to further deepen the results of this investigation and our understanding of self-healing phenomena in HPFRCCs, a micro- and even nano-mechanical characterization of the healing products could, and should, be performed in order to assess and clarify the influence of their nature

and mechanical properties on the observed macroscopical recovery of the mechanical performance of the material.

**Acknowledgments**

The support of Politecnico di Milano – Young Researchers 2011 grant to the project Self-healing capacity of cementitious composites is gratefully acknowledged. The authors also thank Matteo Geminiani, Raffaele Gorlezza and Gregorio Sanchez Arevalo for their help in performing experimental tests along different time steps of the project, in partial fulfilment of the requirements to obtain their MScEng degrees.



**References**

[1] Mihashi, H. and Nishiwaki, T., Development of engineered self-healing and self-repairing concrete: state-of-the-art report, Journal of Advanced Concrete Technology, 10 (2012), 170-184.

[2] Van Tittelboom, K. and De Belie, N., Self-healing in cementitious materials – a review, Materials, 6 (2013), 2182-2217.

[3] European Concrete Societies Network, European Concrete Award 2014, p.13 .

[4] V. Wiktor, H. M. Jonkers, Boelens R., Goedhart J., Jagers S., Oldenkamp R., A concrete solution for a concrete problem, Image Foundation.

[5] Loh G., Microscopic Analysis On The Concrete Cores From Retaining Walls at Changhsi Airport, Terminal 3, Reverton Engineering, Test Report, A6127/chf,

[6] Grant TP (2001). Determination of asphalt mixture healing rate using the Superpave indirect tensile test. Master thesis, University of Florida, America.

Ref, [3] [4], [5] and [6] have been cited by:

[7] Krelani, V., Selg-healing capacity of cementitious composites, *PhD Thesis*, Politecnico di Milano, 2015, 256+xlvi pp.

[8] di Prisco, M., Plizzari, G. and Vandewalle, L., Fiber reinforced concrete. New design perspectives", *Materials and Structures*, 42 (2009), p. 1261-1281.

[9] Ferrara, L., Krelani, V. and Carsana, M., A fracture testing based approach to assess crack healing of concrete with and without crystalline admixtures, *Construction and Building Materials*, 68 (2014), p. 515-531.

[10] Roig-Flores, M., Moscato, S., Serna. P. and Ferrara, L., Self-healing capability of concrete with crystalline admixtures in different environments, *Construction and Building Materials*, 86, 2015, pp. 1-11.

[11] Ferrara, L., Krelani, V., Moretti, F., Roig Flores, M. and Serna Ros, P. (2016), Effects of autogenous healing on the recovery of mechanical performance of High Performance Fibre Reinforced Cementitious Composites (HPFRCCs): part 1, *submitted for publication to Cement and Concrete Composites*, December 13, 2015.

## Tables

**Table 1**. Mix-design of HPFRCC

| Constituent | Dosage (kg/m$^3$) |
|---|---|
| Cement | 600 |
| Slag | 500 |
| Sand (0-2 mm) | 982 |
| Water | 200 |
| Superplasticizer | 33 (l/m$^3$) |
| Straight steel fibres ($l_f$ = 13 mm; $d_f$ = 0.16 mm) | 100 |

**Table 2.**

| | | Deflection behaviour | | | | | | | | | | | |
|---|---|---|---|---|---|---|---|---|---|---|---|---|---|
| | | Softening | | | Hardening | | | | | | | | |
| Pre-crack opening | | 0.5 mm | | | 1 mm | | | 2 mm | | | $COD_{peak}$ + 0.5 mm | | |
| Exposure duration (months) | | 1 | 6 | 24 | 1 | 6 | 24 | 1 | 6 | 24 | 1 | 6 | 24 |
| Exposure Conditions | Water immersion | *1* | *2* | *1* | *1* | *1* | *1* | *2* | *1* | *2* | *2* | *2* | *2* |
| | Air exposure | *1* | *2* | *1* | *1* | *1* | *1* | *2* | *1* | *2* | *2* | *2* | *1* |
| | 20°C – RH = 90% | *1* | *2* | *1* | *1* | *1* | *1* | *2* | *1* | *2* | *2* | *2* | *2* |
| | 20°C – RH = 50% | *1* | *=* | *2* | *1* | *1* | *1* | *2* | *4* | *2* | *2* | *2* | *2* |
| | Wet and dry | *1* | *2* | *2* | *1* | *1* | *1* | *2* | *2* | *1* | *2* | *2* | *2* |

Synopsis of the experimental program: number of specimens tested per each exposure condition and duration, deflection hardening/softening behaviour and pre-crack opening (**Age of pre-crack of 2 months**).

| | | Deflection behaviour | | | | | | | | | | | | | | | |
|---|---|---|---|---|---|---|---|---|---|---|---|---|---|---|---|---|---|
| | | Softening | | | | Hardening | | | | | | | | | | | |
| Pre-crack opening | | 0.5 mm | | | | 1 mm | | | | 2 mm | | | | $COD_{peak}$ + 0.5 mm | | | |
| Exposure duration (months) | | 1 | 3 | 6 | 24 | 1 | 3 | 6 | 24 | 1 | 3 | 6 | 24 | 1 | 3 | 6 | 24 |
| Age of pre-crack | 2 months | *1* | | *2* | *1* | *1* | | *1* | *1* | *2* | | *1* | *2* | *2* | | *2* | *2* |
| | 11 months | *3* | *2* | *3* | | *1* | *1* | *=* | | *1* | *1* | *1* | | *1* | *1* | *1* | |

Synopsis of the experimental program: number of specimens tested per each exposure duration, age of pre-cracking, deflection hardening/softening behaviour and pre-crack opening (**Exposure Conditions Water immersion**).

**Table 3.** Indices of recovery of mechanical properties and of crack healing for all tested specimens (next pages).

| | pre crack opening | Conditioning time (months) | ISR | IDuR pre-peak | IDaR | IDuR post-peak | ICH damage | ICH av. crack |
|---|---|---|---|---|---|---|---|---|
| Water immersion – pre-cracked at 11 months | 1 mm | 1 | 73% | 92% | 80% | 55% | 62% | 68% |
| | 1 mm | 3 | 146% | 30% | 40% | 108% | 52% | 92% |
| | 2 mm | 1 | 79% | 7% | 42% | 98% | 55% | 70% |
| | 2 mm | 3 | 495% | 69% | 38% | 104% | 54% | 83% |
| | 2 mm | 6 | 1258% | 48% | 63% | 103% | 68% | 89% |
| | 0.5 mm post-peak | 1 | 70% | -80% | 39% | 56% | 51% | 49% |
| | 0.5 mm post-peak | 3 | 631% | -14% | 72% | 74% | 67% | 81% |
| | 0.5 mm post-peak | 6 | 831% | -72% | 72% | 61% | 72% | 91% |
| | 0.5 mm | 1 | 41% | - | 7% | - | 25% | 49% |
| | 0.5 mm | 1 | 20% | - | -68% | - | -25% | 70% |
| | 0.5 mm | 1 | 33% | - | 22% | - | 12% | 16% |
| | 0.5 mm | 1 | 46% | - | 33% | - | 44% | 0% |
| | 0.5 mm | 3 | 54% | - | 35% | - | 35% | 98% |
| | 0.5 mm | 3 | 18% | - | 10% | - | 17% | 72% |
| | 0.5 mm | 6 | 77% | - | 78% | - | 66% | 92% |
| | 0.5 mm | 6 | 46% | - | 44% | - | 51% | 92% |

| | pre crack opening | Conditioning time (months) | ISR | IDuR pre-peak | IDaR | IDuR post-peak | ICH damage | ICH av. crack |
|---|---|---|---|---|---|---|---|---|
| Water immersion – precracked at 2 months | 1 mm | 1 | 236% | -5% | 106% | 63% | 68% | 0% |
| | 1 mm | 6 | 347% | -1% | 67% | 50% | 64% | 100% |
| | 1 mm | 24 | 528% | -13% | 179% | 29% | 78% | 100% |
| | 2 mm | 1 | 232% | 3% | 41% | 60% | 78% | 100% |
| | 2 mm | 1 | 329% | 20% | 34% | 93% | 78% | 100% |
| | 2 mm | 6 | 1237% | 53% | 51% | 42% | 84% | 100% |
| | 2 mm | 24 | 1111% | -5% | 111% | 27% | 81% | 100% |
| | 0.5 mm post-peak | 1 | 816% | 125% | 35% | 135% | 80% | 81% |
| | 0.5 mm post-peak | 1 | 855% | 33% | 9% | 26% | 87% | 80% |
| | 0.5 mm post-peak | 6 | 3342% | 63% | -10% | 9% | 80% | 97% |
| | 0.5 mm post-peak | 6 | 4788% | 147% | 38% | 29% | 78% | 0% |
| | 0.5 mm post-peak | 24 | 2293% | 42% | 68% | 13% | 88% | 100% |
| | 0.5 mm post-peak | 24 | 2005% | 64% | 85% | 17% | 86% | 100% |
| | 0.5 mm | 1 | 26% | - | 14% | - | 57% | 90% |
| | 0.5 mm | 6 | 78% | - | 50% | - | 56% | 84% |
| | 0.5 mm | 6 | 93% | - | 122% | - | 43% | 100% |

| | pre crack opening | Conditioning time (months) | ISR | IDuR pre-peak | IDaR | IDuR post-peak | ICH damage | ICH av. crack |
|---|---|---|---|---|---|---|---|---|
| Air immersion | 1 mm | 1 | 47% | 175% | -49% | 50% | -4% | 4% |
| | 1 mm | 6 | 95% | 92% | 55% | 32% | 64% | 85% |
| | 1 mm | 24 | 126% | 62% | 167% | 20% | 74% | 70% |
| | 2 mm | 1 | 169% | 174% | 3% | 49% | 63% | 10% |
| | 2 mm | 1 | 183% | 190% | 39% | 62% | 77% | 26% |
| | 2 mm | 6 | 444% | 173% | 6% | 70% | 72% | 38% |
| | 2 mm | 24 | 687% | 132% | 99% | 19% | 79% | 79% |
| | 2 mm | 24 | 763% | 122% | 199% | 24% | 83% | 83% |
| | 0.5 mm post-peak | 1 | 112% | 37% | 10% | 98% | 75% | 27% |
| | 0.5 mm post-peak | 1 | 301% | -8% | -15% | 140% | 78% | 12% |
| | 0.5 mm post-peak | 6 | 408% | 47% | 11% | 66% | 77% | 49% |
| | 0.5 mm post-peak | 6 | 516% | 61% | -19% | 66% | 85% | 47% |
| | 0.5 mm post-peak | 24 | 1336% | 46% | 96% | 21% | 85% | 59% |
| | 0.5 mm | 1 | 48% | - | 48% | - | 42% | 7% |
| | 0.5 mm | 6 | 187% | - | 78% | - | 58% | 60% |
| | 0.5 mm | 6 | 129% | - | 19% | - | 31% | 42% |
| | 0.5 mm | 24 | 47% | -35% | 268% | 27% | 79% | 47% |

| Humid chamber (RH 90%) | pre crack opening | Conditioning time (months) | ISR | IDuR pre-peak | IDaR | IDuR post-peak | ICH damage | ICH av. crack |
|---|---|---|---|---|---|---|---|---|
| | 1 mm | 1 | 35% | 18% | 19% | 129% | 48% | 18% |
| | 1 mm | 6 | 99% | 31% | 28% | 198% | 54% | 16% |
| | 1 mm | 24 | 199% | 0% | 172% | 23% | 74% | 92% |
| | 2 mm | 1 | 173% | 19% | 94% | 164% | 83% | 14% |
| | 2 mm | 1 | 172% | 28% | 9% | 54% | 71% | 33% |
| | 2 mm | 6 | 367% | 6% | -7% | 161% | 67% | 12% |
| | 2 mm | 24 | 700% | 12% | 72% | 84% | 78% | 40% |
| | 2 mm | 24 | 757% | 8% | 107% | 109% | 79% | 79% |
| | 0.5 mm post-peak | 1 | 276% | 78% | -39% | 181% | 74% | 4% |
| | 0.5 mm post-peak | 1 | 189% | 42% | -16% | 51% | 77% | 14% |
| | 0.5 mm post-peak | 6 | 330% | 62% | -21% | 142% | 71% | 30% |
| | 0.5 mm post-peak | 6 | 265% | 16% | -18% | 97% | 74% | 22% |
| | 0.5 mm post-peak | 24 | 841% | 38% | 73% | 70% | 84% | 22% |
| | 0.5 mm post-peak | 24 | 547% | 30% | 27% | 60% | 80% | 48% |
| | 0.5 mm | 1 | 64% | - | 41% | - | 55% | 16% |
| | 0.5 mm | 6 | 49% | - | 38% | - | 73% | 38% |
| | 0.5 mm | 6 | 81% | - | 39% | - | 51% | 16% |
| | 0.5 mm | 24 | 117% | - | 209% | - | 66% | 2% |

| Dry chamber (RH 50%) | pre crack opening | Conditioning time (months) | ISR | IDuR pre-peak | IDaR | IDuR post-peak | ICH damage | ICH av. crack |
|---|---|---|---|---|---|---|---|---|
| | 1 mm | 1 | 48% | 3% | 6% | 143% | 51% | 18% |
| | 1 mm | 6 | 119% | 68% | 1% | 142% | 50% | 19% |
| | 1 mm | 24 | 44% | -13% | 50% | 112% | 61% | 10% |
| | 2 mm | 1 | 394% | 53% | -3% | 169% | 68% | 15% |
| | 2 mm | 1 | 128% | 12% | -6% | 130% | 68% | 17% |
| | 2 mm | 6 | 254% | 21% | 9% | 234% | 70% | 9% |
| | 2 mm | 6 | 42% | -11% | -40% | 221% | 38% | 13% |
| | 2 mm | 6 | 122% | 3% | -7% | 229% | 62% | 9% |
| | 2 mm | 6 | -23% | -15% | -17% | 222% | 59% | 25% |
| | 2 mm | 24 | 235% | -7% | 52% | 82% | 80% | 23% |
| | 2 mm | 24 | 370% | 9% | 16% | 114% | 70% | 12% |
| | 0.5 mm post-peak | 1 | 6% | 26% | -27% | 82% | 71% | 6% |
| | 0.5 mm post-peak | 1 | 6% | 20% | -5% | 62% | 74% | 11% |
| | 0.5 mm post-peak | 6 | 107% | 116% | -24% | 50% | 71% | 10% |
| | 0.5 mm post-peak | 6 | 105% | 40% | 4% | 37% | 64% | 15% |
| | 0.5 mm post-peak | 24 | 279% | 35% | -5% | 168% | 73% | 8% |
| | 0.5 mm post-peak | 24 | 26% | 12% | 201% | 422% | 87% | 7% |
| | 0.5 mm | 1 | -53% | -75% | 49% | 171% | 58% | 6% |
| | 0.5 mm | 24 | 9% | -50% | 110% | 15% | 64% | 31% |
| | 0.5 mm | 24 | 40% | -26% | 0% | 90% | 65% | 39% |

| | pre crack opening | Conditioning time (months) | ISR | IDuR pre-peak | IDaR | IDuR post-peak | ICH damage | ICH av. crack |
|---|---|---|---|---|---|---|---|---|
| Wet and dry cycles (water-50%RH) | 1 mm | 1 | 87% | 64% | 44% | 218% | 53% | |
| | 1 mm | 6 | 185% | 225% | 82% | 39% | 68% | 98% |
| | 1 mm | 24 | 188% | -6% | 141% | 43% | 74% | 100% |
| | 1 mm | 24 | 125% | -4% | 119% | 109% | 87% | 100% |
| | 2 mm | 1 | 307% | 46% | 58% | 169% | 75% | |
| | 2 mm | 1 | 353% | 74% | -333% | 187% | 41% | |
| | 2 mm | 6 | 753% | 230% | 19% | 37% | 74% | 100% |
| | 2 mm | 6 | 691% | 455% | 46% | 67% | 80% | 100% |
| | 2 mm | 24 | 877% | 35% | 124% | 98% | 78% | 100% |
| | 0.5 mm post-peak | 1 | 391% | 43% | 10% | 61% | 78% | |
| | 0.5 mm post-peak | 1 | 469% | 38% | 6% | 147% | 80% | |
| | 0.5 mm post-peak | 6 | 1635% | 75% | 34% | 54% | 86% | 98% |
| | 0.5 mm post-peak | 6 | 553% | 61% | 18% | 58% | 85% | 88% |
| | 0.5 mm post-peak | 24 | 984% | 35% | 89% | 52% | 89% | 95% |
| | 0.5 mm post-peak | 24 | 561% | 29% | 98% | 79% | 90% | 99% |
| | 0.5 mm | 1 | -94% | -91% | 851% | 21% | 20% | |
| | 0.5 mm | 6 | 42% | - | 65% | - | 53% | 85% |
| | 0.5 mm | 6 | 35% | - | 41% | - | 45% | 88% |
| | 0.5 mm | 24 | 35% | - | 293% | - | 50% | 100% |
| | 0.5 mm | 24 | -81% | -43% | 380% | 165% | 50% | 100% |

**Figures**

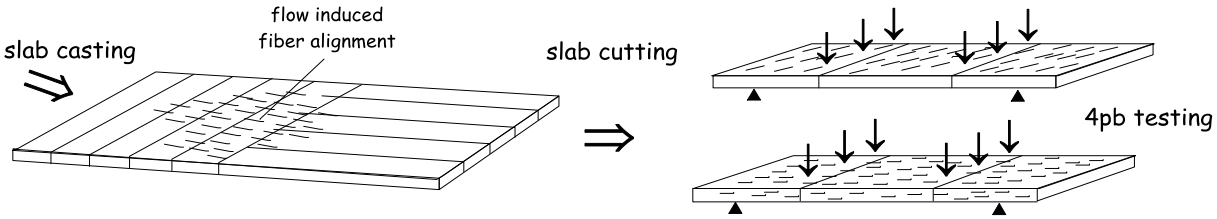


slab cutting and specimen cutting procedure

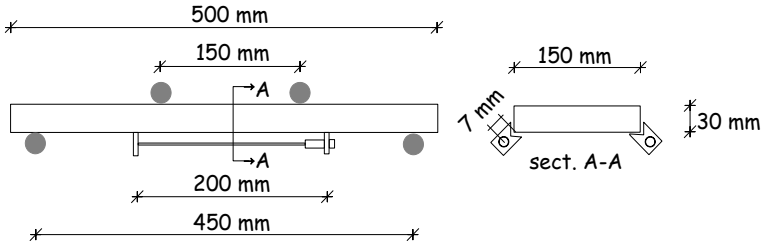


pre-cracking 4pb test

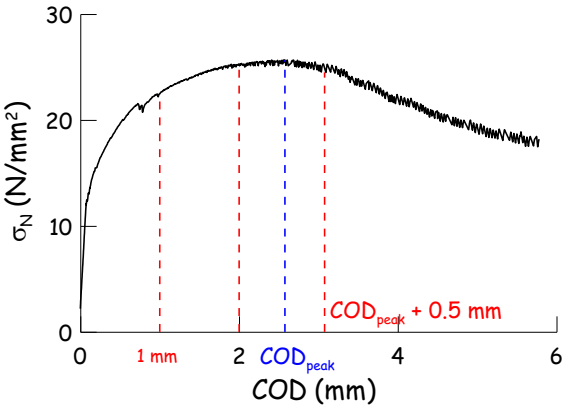


Deflection hardening

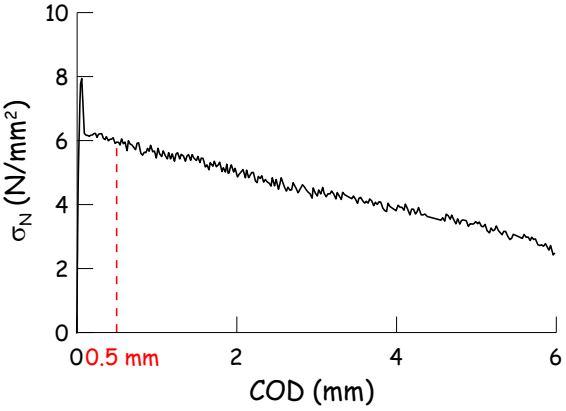


Deflection softening

Environmental conditioning

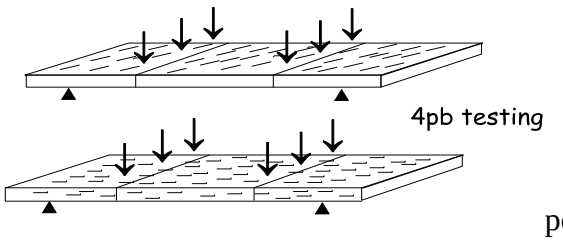


post-conditioning failure tests

**Figure 1.** Schematic of the experimental programme.

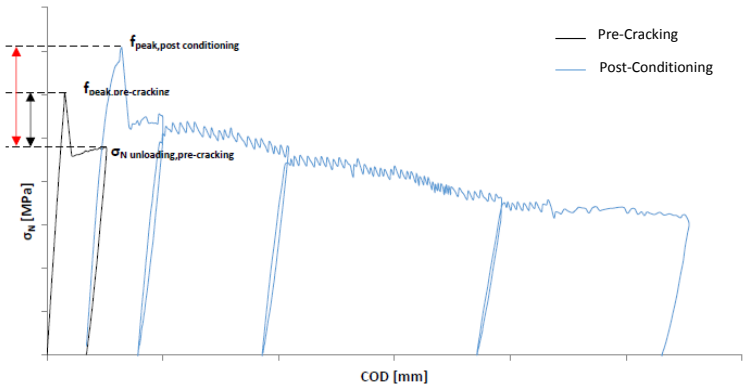


(a)

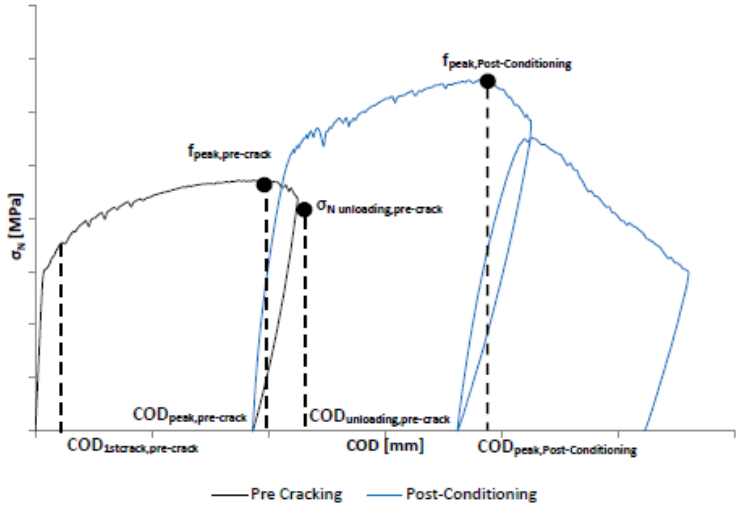


(b)

Index of Strength Recovery ISR = $\dfrac{f_{peak,post conditioning} - \sigma_{N\ unloading pre-cracking}}{f_{peak,pre-cracking} - \sigma_{N\ unloading pre-cracking}}$ (for a and b)

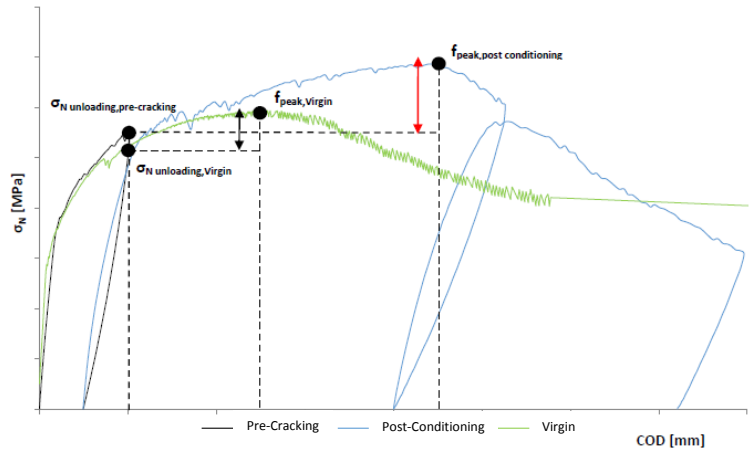


(c)

Index of Strength Recovery ISR = $\dfrac{\left(f_{peak,post-conditioning} - \sigma_{N\ unloainhg pre-crack}\right)}{\left(f_{peak,virgin} - \sigma_{N,unloading,virgin}\right)} \dfrac{\sigma_{N,unloading,virgin}}{\sigma_{N,unloading pre-crack}} - 1$ (for c)

**Figure 2.** Notation and definition of the Index of Strength Recovery for deflection softening specimens (a) and deflection hardening specimens pre-cracked after (b) or before the peak (c).

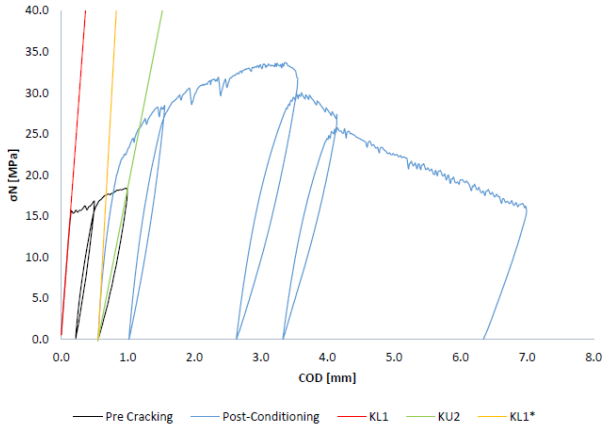


$$\text{Index of Damage Recovery IDaR} = \frac{K_{reloading,postconditoning} - K_{\text{unloadingpre-cracking}}}{K_{loading,pre-cracking} - K_{\text{unloadingpre-cracking}}}$$

**Figure 3:** notation and definition of the Index of Damage Recovery.

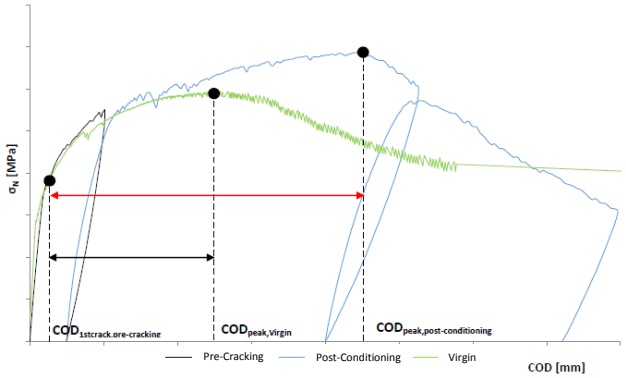


(a)

$$\text{Index of Ductility Recovery IDuR} = \frac{\left(COD_{peak,post-conditioning} - COD_{1st\ crack,pre-crack}\right)}{\left(COD_{peak,virgin} - COD_{1stcrack,virgin}\right)} \quad -1$$

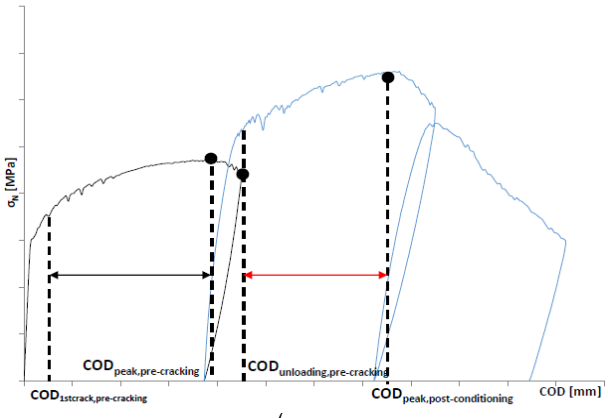


(b)

$$\text{Index of Ductility Recovery IDuR} = \frac{\left(COD_{peak,post-conditioning} - COD_{unloading,pre-crack}\right)}{\left(COD_{peak,pre-crack} - COD_{1stcrack,pre-crack}\right)}$$

**Figure 4.** Notation and definition of the Index of Ductility Recovery for deflection-hardening specimens pre-cracked in the pre-peak (a) and post-peak regime (b).

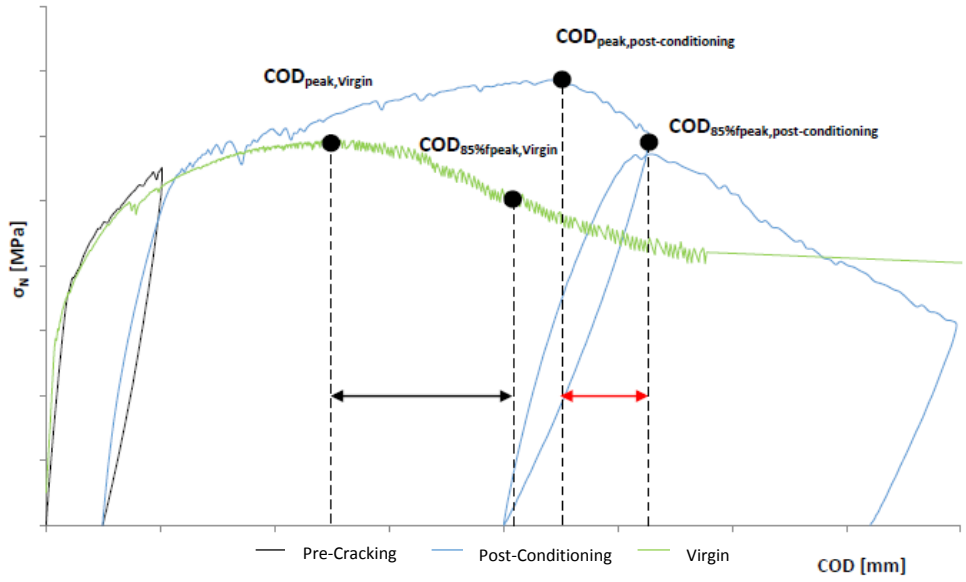


(a)

$$\mathrm{IDuR}_{\text{post-peak}} = \frac{\left(COD_{85\%\,peak,post-conditioning} - COD_{peak,post-conditioning}\right)}{\left(COD_{85\%\,peak,virgin} - COD_{peak,virgin}\right)}$$

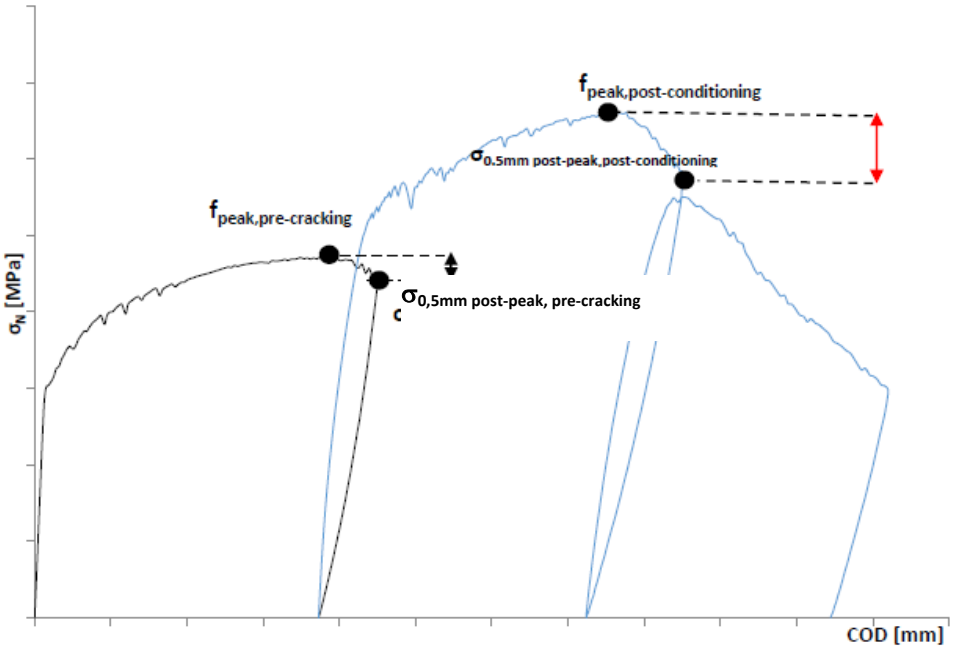


(b)

$$\mathrm{IDuR}_{\text{post-peak}} = \frac{\left(f_{peak,post-conditioning} - \sigma_{0.5mm\ post-peak,post-conditioning}\right)}{\left(f_{peak,pre-cracking} - \sigma_{0.5mm\ post-peak,pre-cracking}\right)}$$

**Figure 5.** Notation and definition of the Index of post-peak Ductility Recovery for deflection-hardening specimens pre-cracked in the pre-peak (a) and post-peak regime (b).


(a)

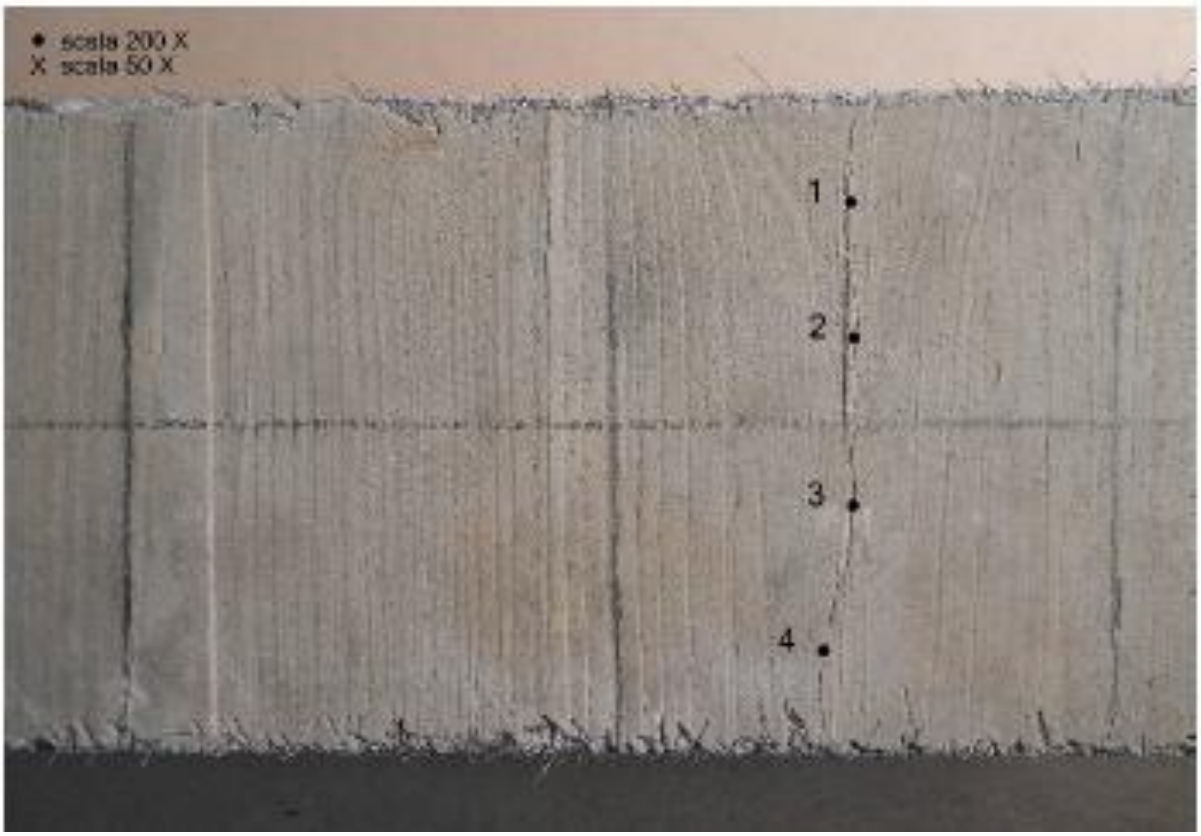


(b)

**Figure 6.** Examples of photographic mapping of cracks and location of magnified images locations.

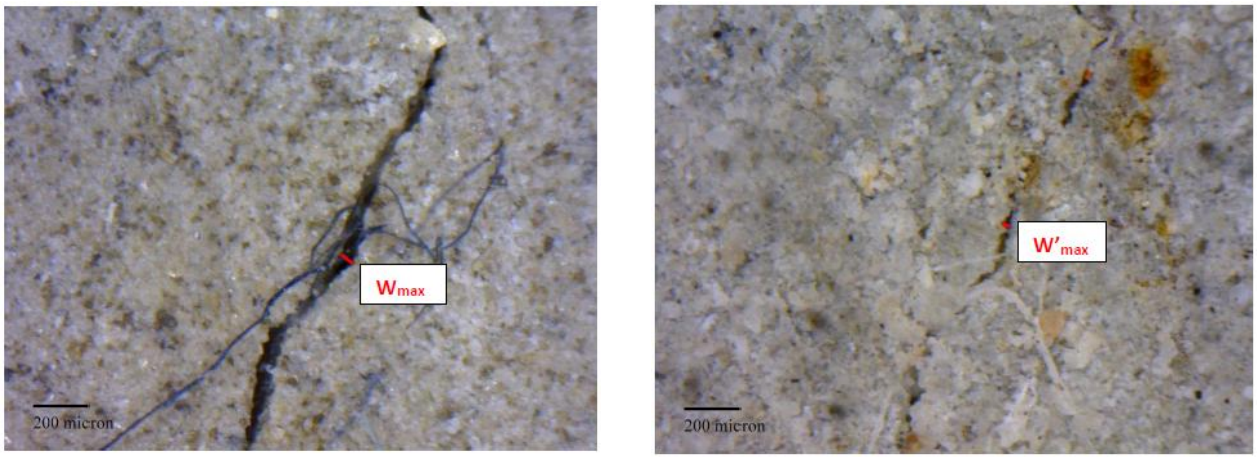


A - Maximum crack width before (left) and after conditioning (rigth)

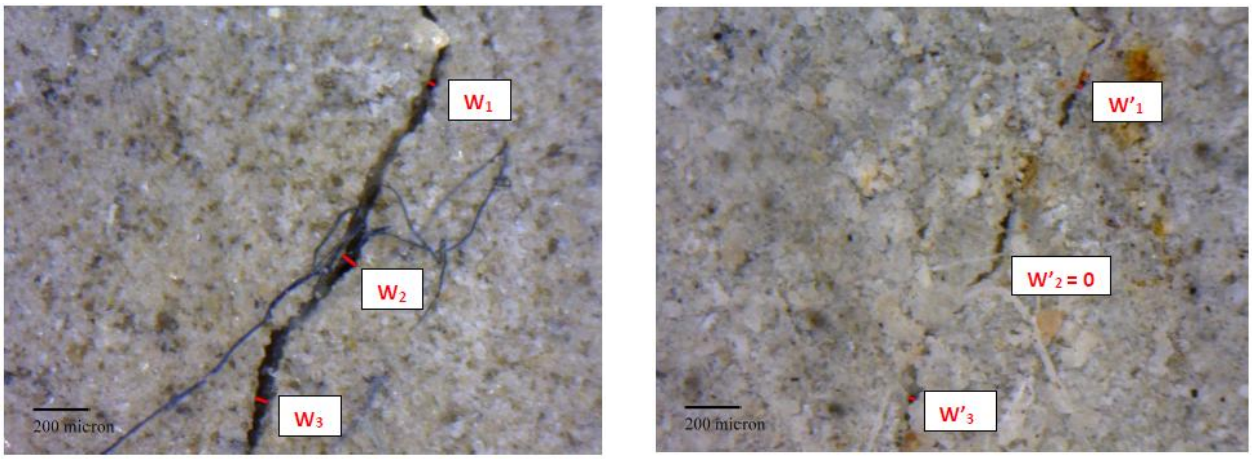


B- Measure points for calculation of average crack width before (left) and after conditioning (right)

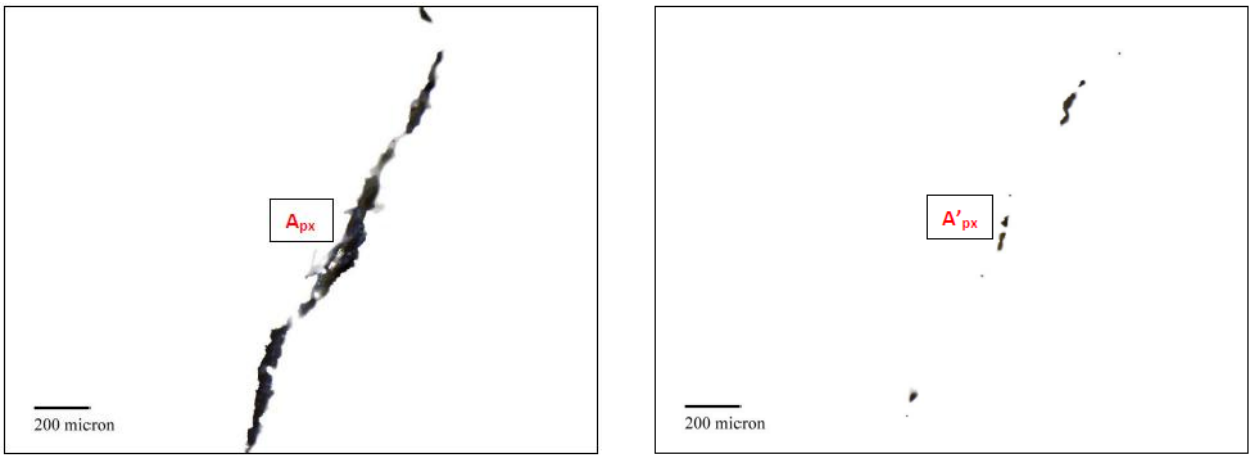


C – filtered crack images for pixel area evaluation before (left) and after conditioning (rigth)

**Figure 7.** Example of visual image processing for evaluation of crack closure due to self-healing phenomena: maximum crack width (a), average crack width (b) and pixel area (c).

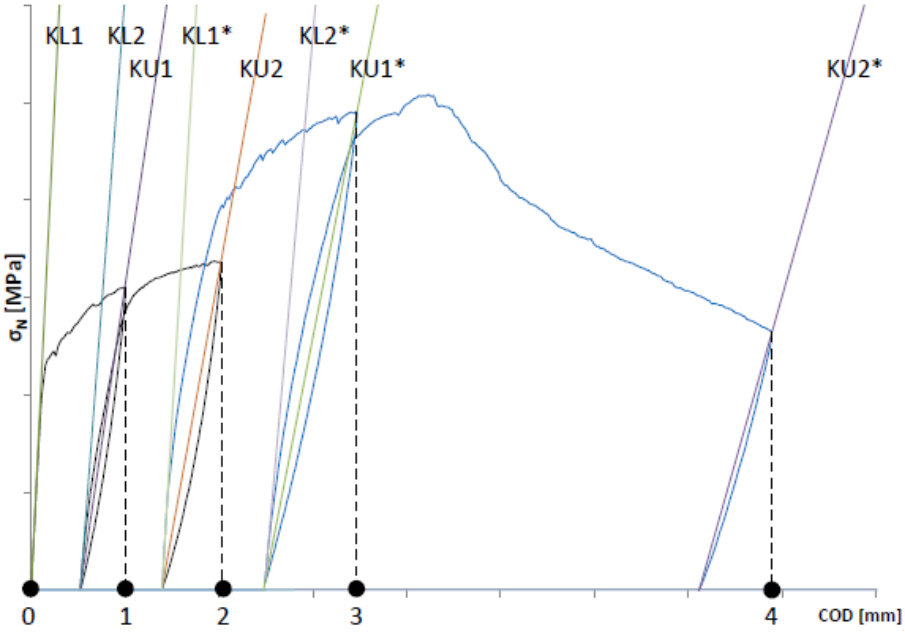


| 4pb test | Damage | | COD | 4pb test | Damage | | COD |
|---|---|---|---|---|---|---|---|
| Pre-cracking | D1 | $1-\frac{K_{U1}}{K_{L1}}$ | 1 | Post conditioning | D3 | $1-\frac{K_{L1*}}{K_{L1}}$ | 2 |
| | D2 | $1-\frac{K_{U2}}{K_{L1}}$ | 2 | | D4 | $1-\frac{K_{U1*}}{K_{L1}}$ | 3 |
| | | | | | D5 | $1-\frac{K_{U2*}}{K_{L1}}$ | 4 |

**Figure 8.** Notation and definition for the construction of Damage vs. COD evolution curves.

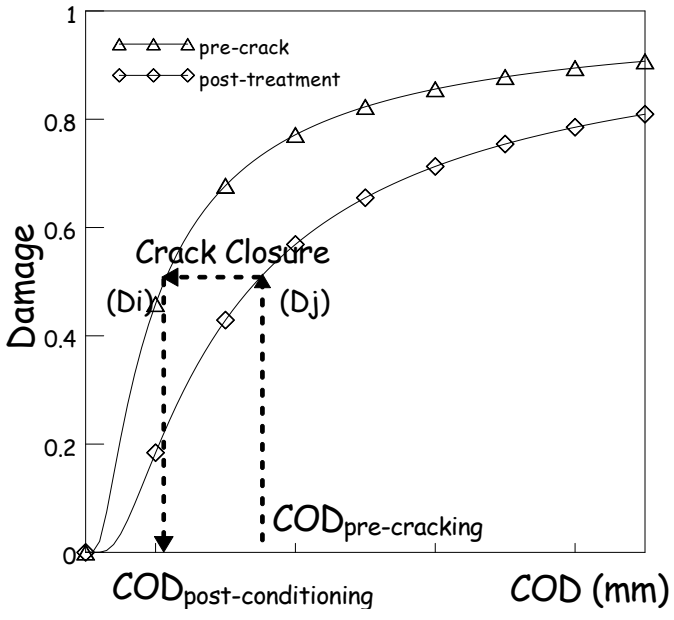


**Figure 10.** Example of damage evolution curves with crack closure evaluation.

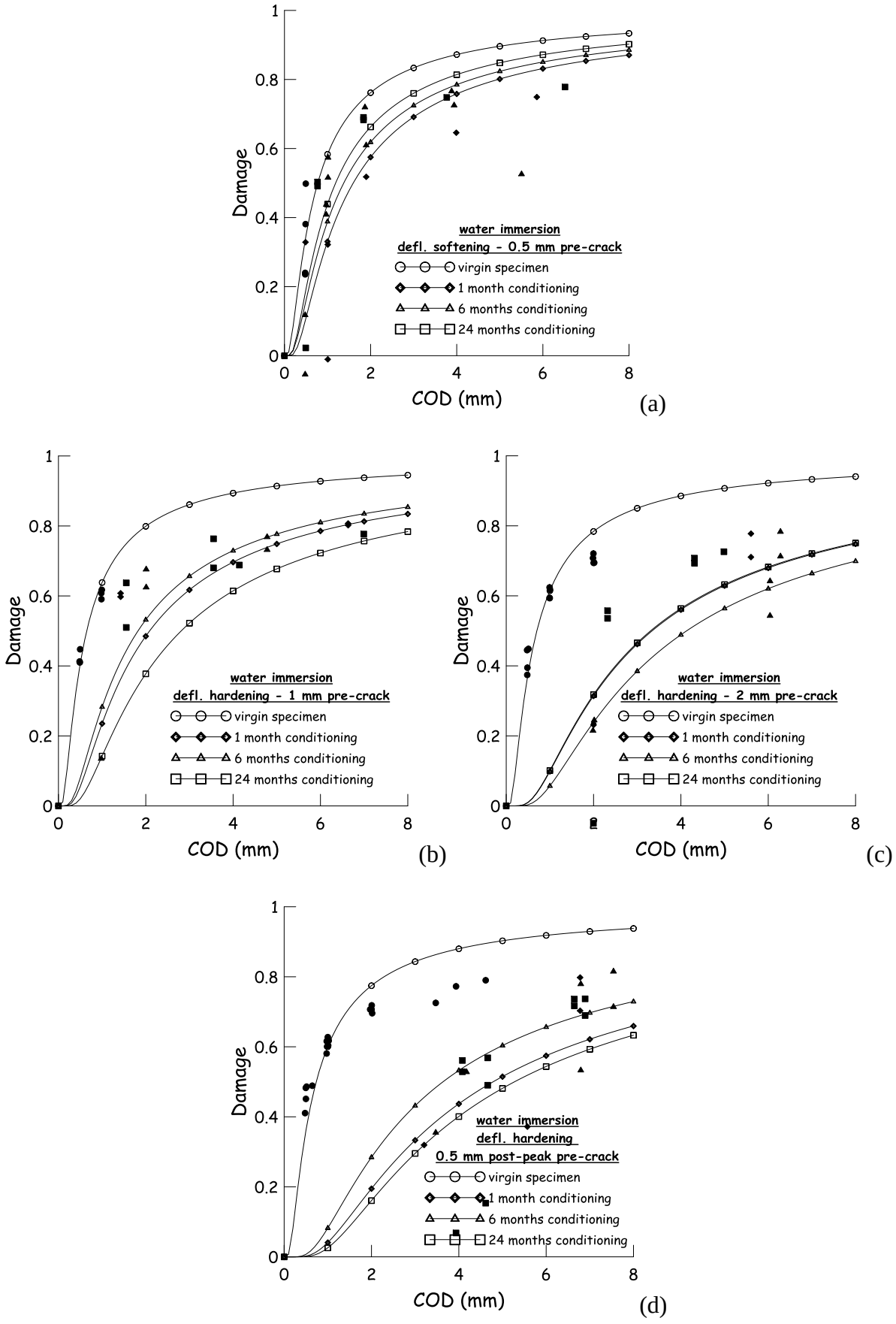


**Figure 9 a-d:** pre-crack and post-conditioning damage evolution curves for deflection softening (a) and hardening (b-d) specimens immersed in water – pre-cracking age 2 months;

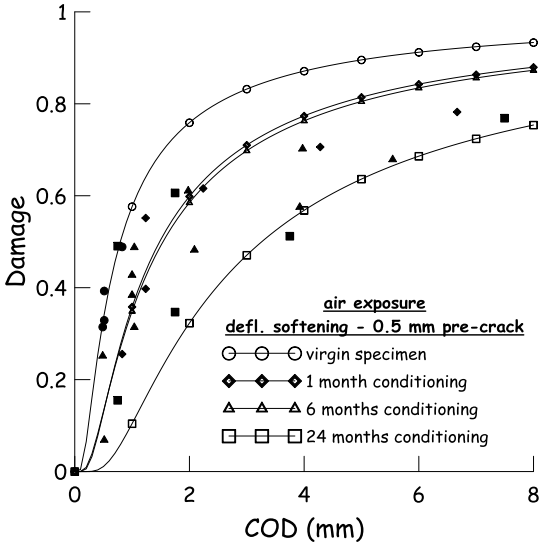


(e)

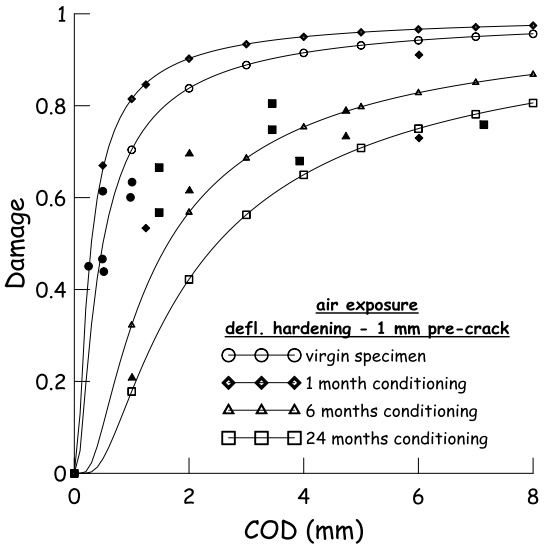


(f)

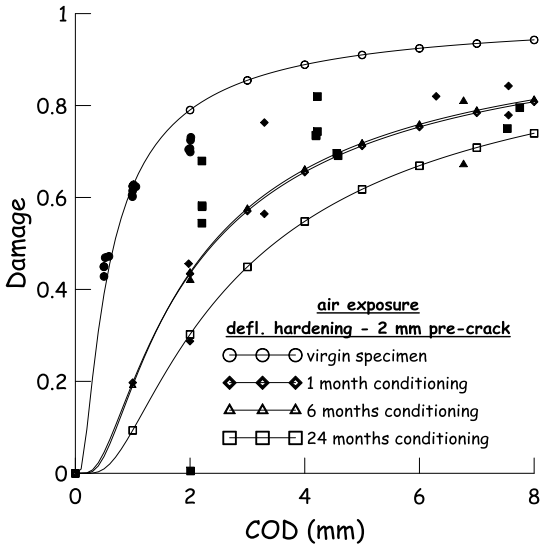


(g)

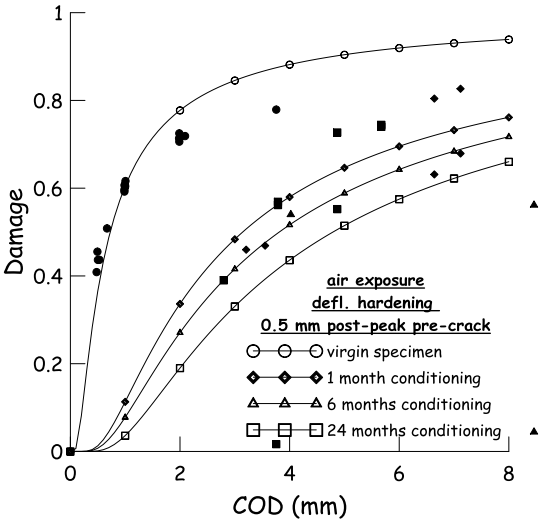


(h)

**Figure 9 e-h:** pre-crack and post-conditioning damage evolution curves for deflection softening (e) and hardening (f-h) specimens exposed to open air – pre-cracking age 2 months;

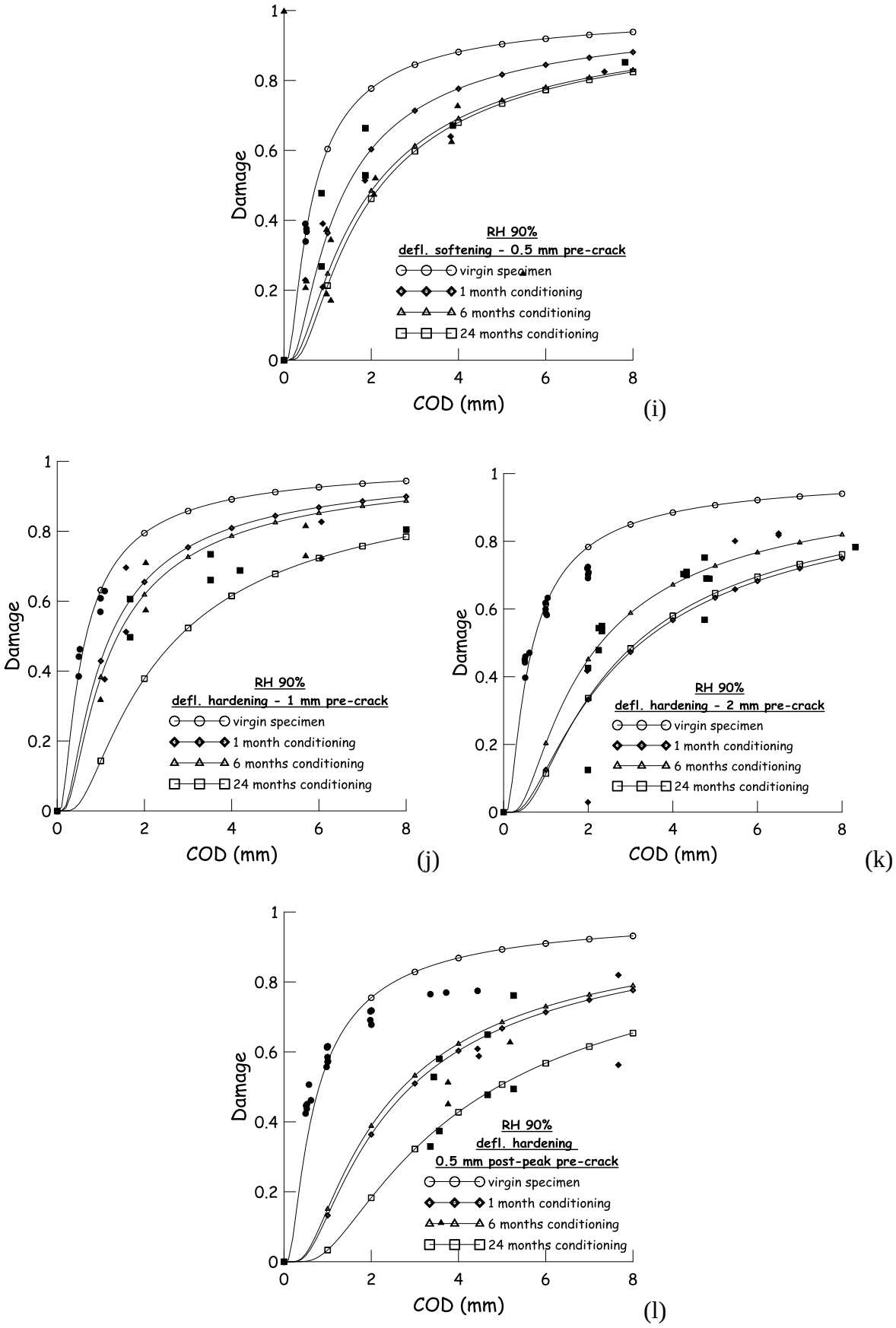


**Figure 9 i-l:** pre-crack and post-conditioning damage evolution curves for deflection softening (i) and hardening (j-l) specimens exposed to 90% RH – pre-cracking age 2 months;

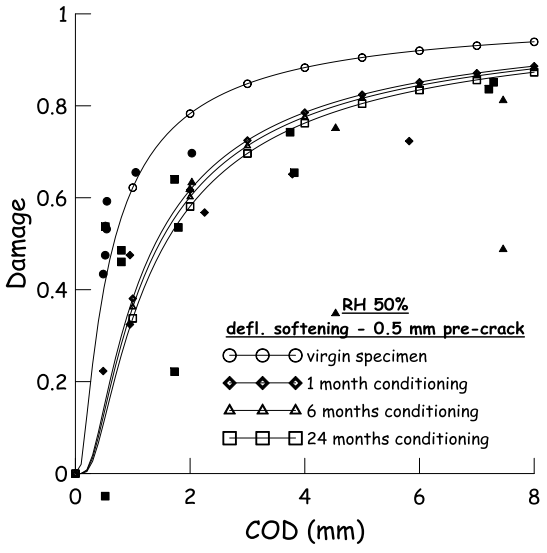


(m)

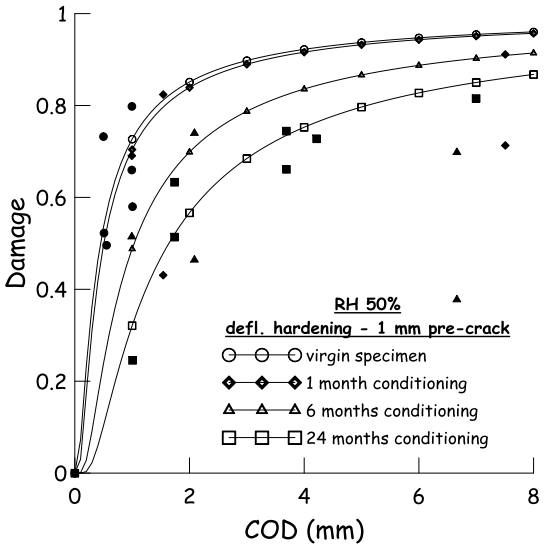


(n)

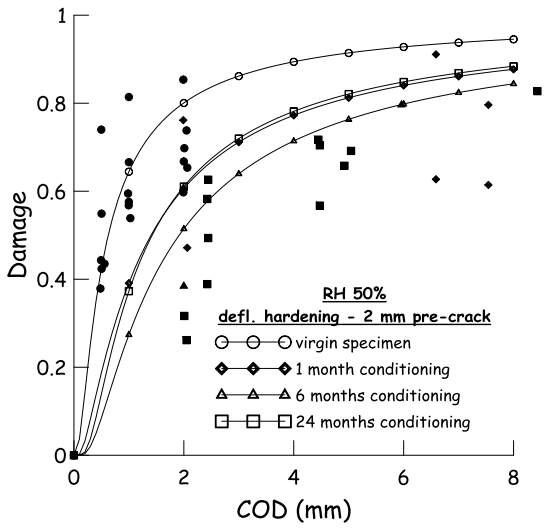


(o)

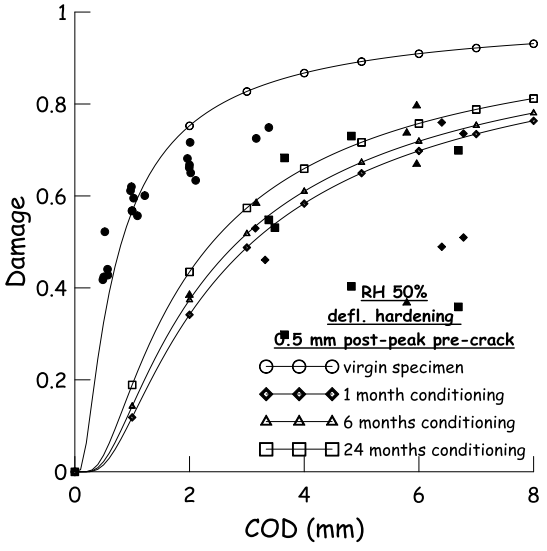


(p)

**Figure 9 m-p:** pre-crack and post-conditioning damage evolution curves for deflection softening (m) and hardening (n-p) specimens exposed to 50% RH – pre-cracking age 2 months;

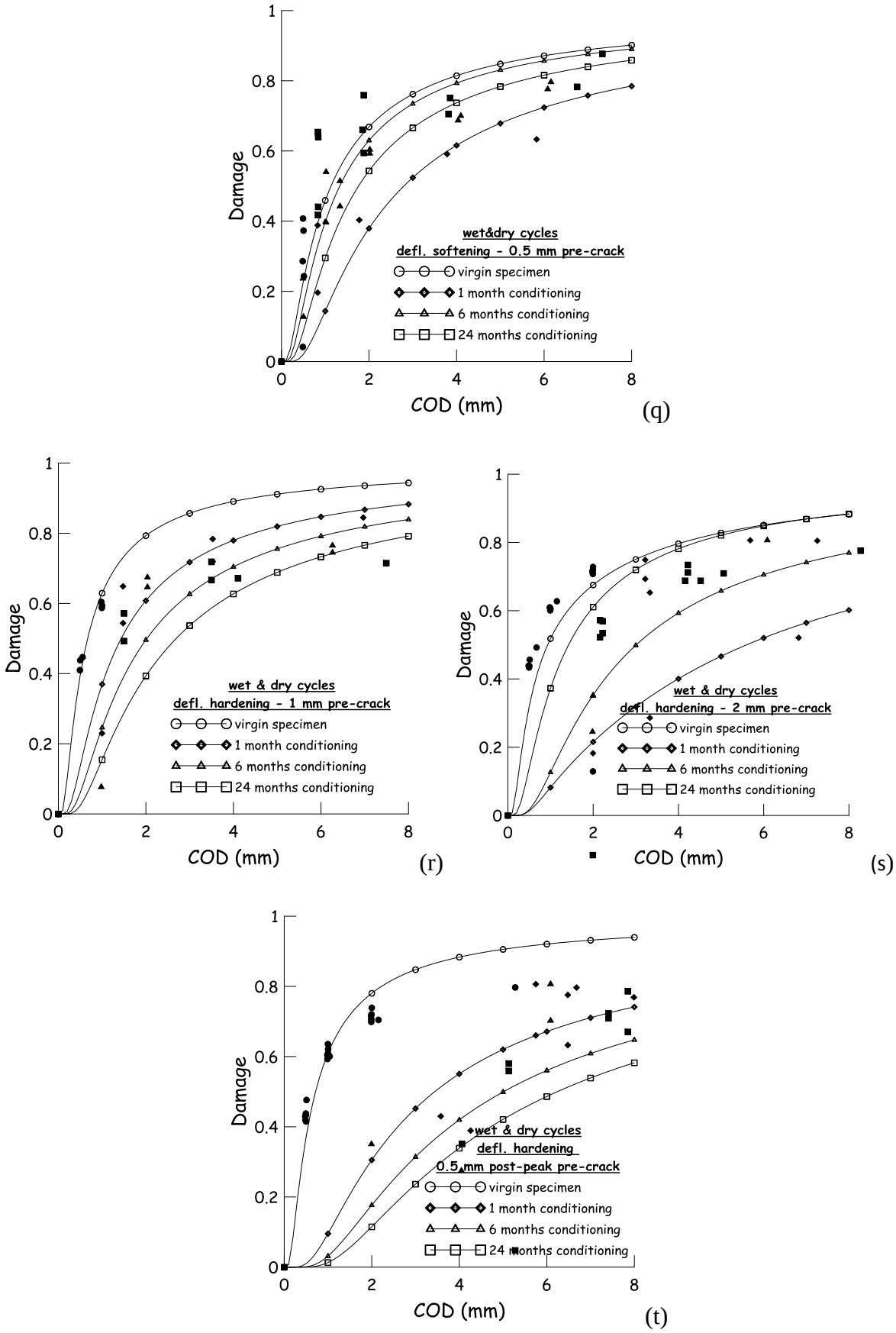


**Figure 9 q-t:** pre-crack and post-conditioning damage evolution curves for deflection softening (q) and hardening (r-t) specimens exposed to wet and dry cycles – pre-cracking age 2 months;

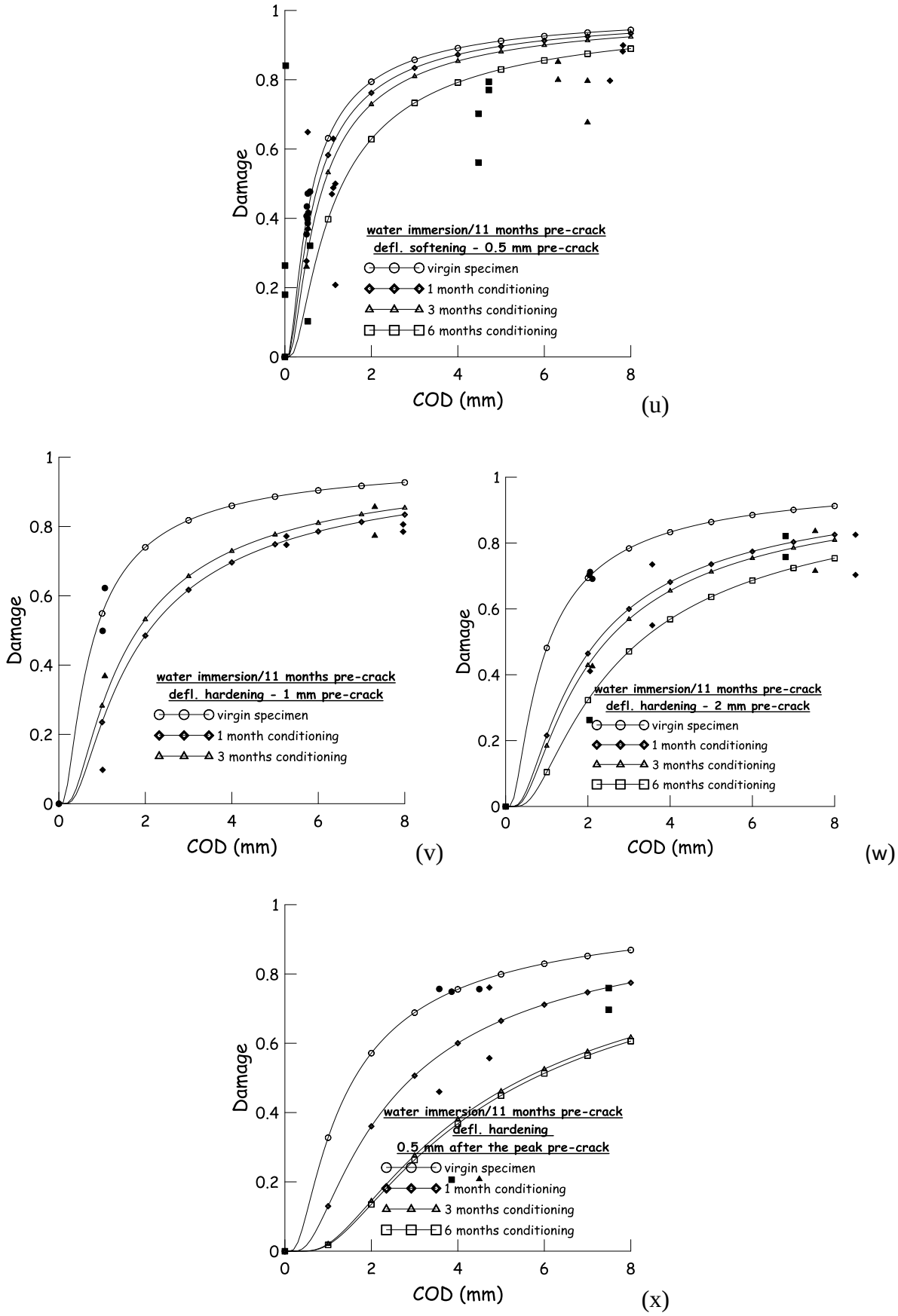


**Figure 9 u-x:** pre-crack and post-conditioning damage evolution curves for deflection softening (u) and hardening (v-x) specimens immersed in water – pre-cracking age 11 months;

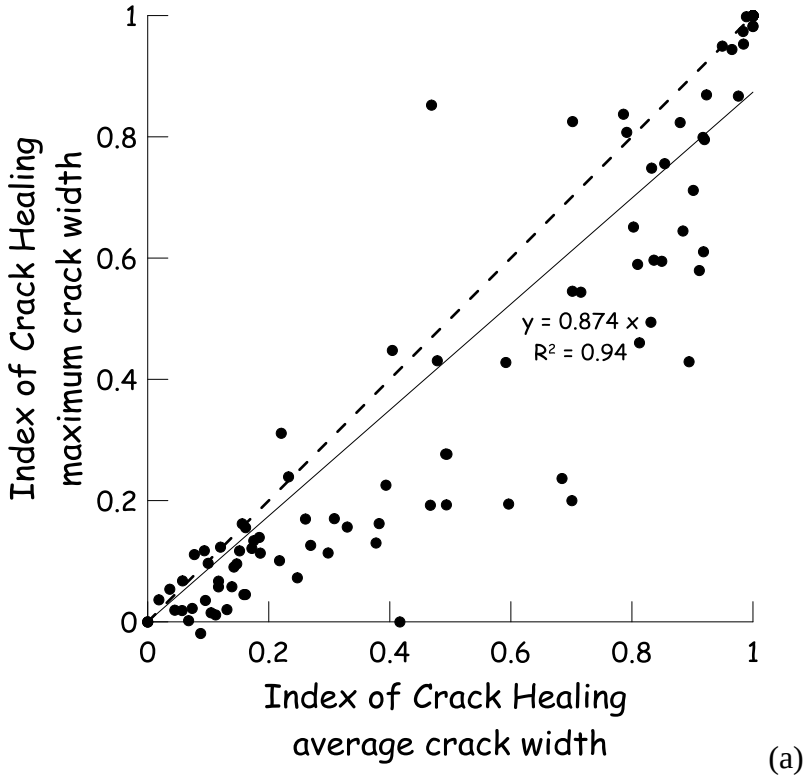


(a)

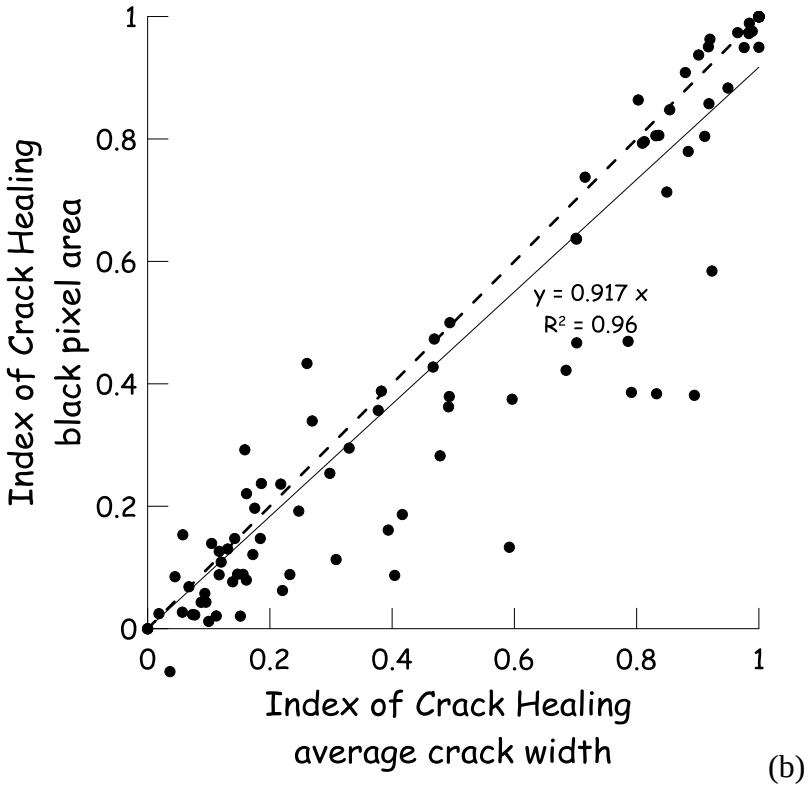


(b)

**Figure 11:** correlation between Index of Crack Healing as per maximum crack width (a) and per black area pixel (b) vs. the Index of Crack Healing as per average crack width.

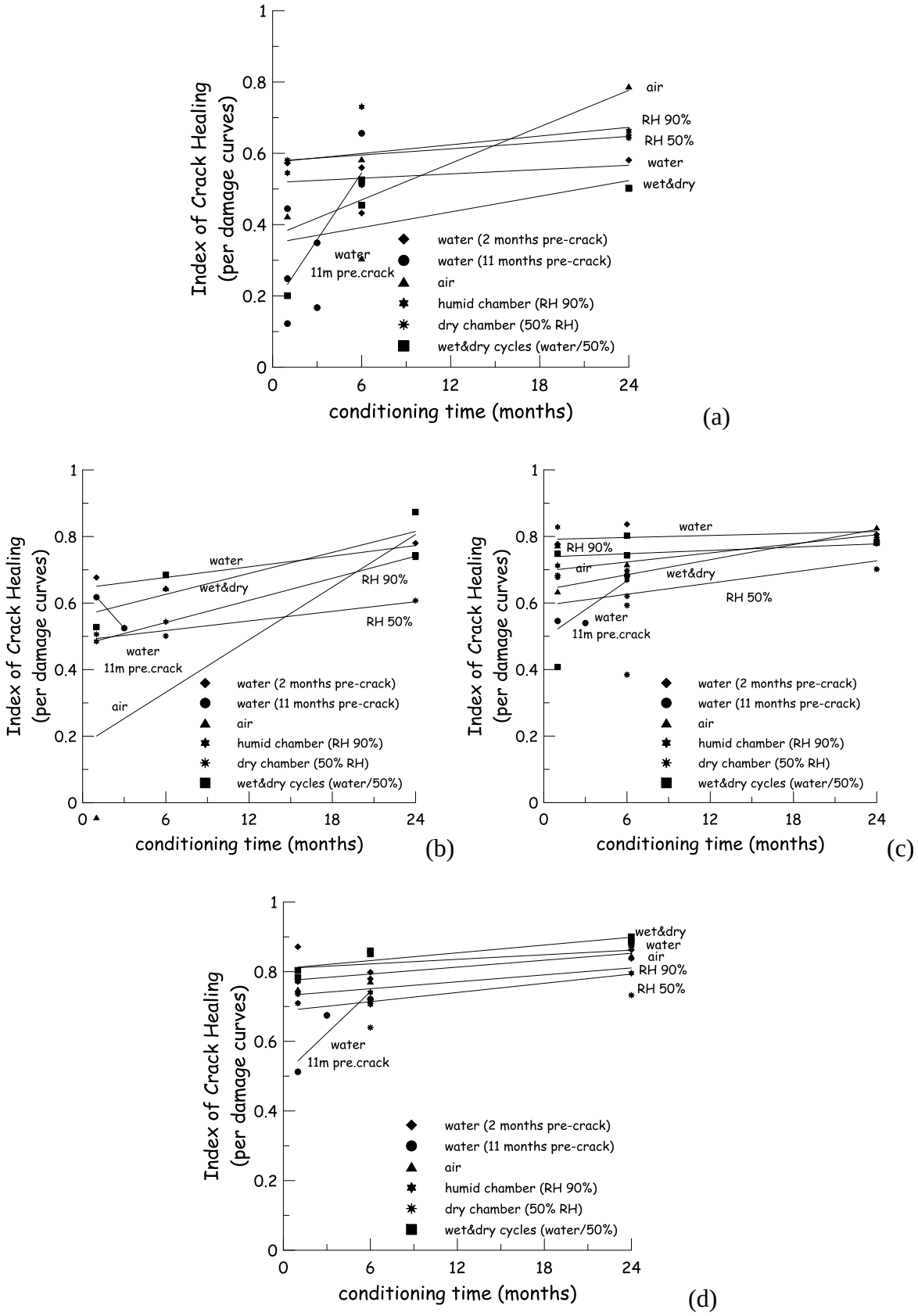


**Figure 12:** Index of Crack Healing, as per damage evolution curves, vs. conditioning time for deflection softening (a) and hardening (b-d) specimens.

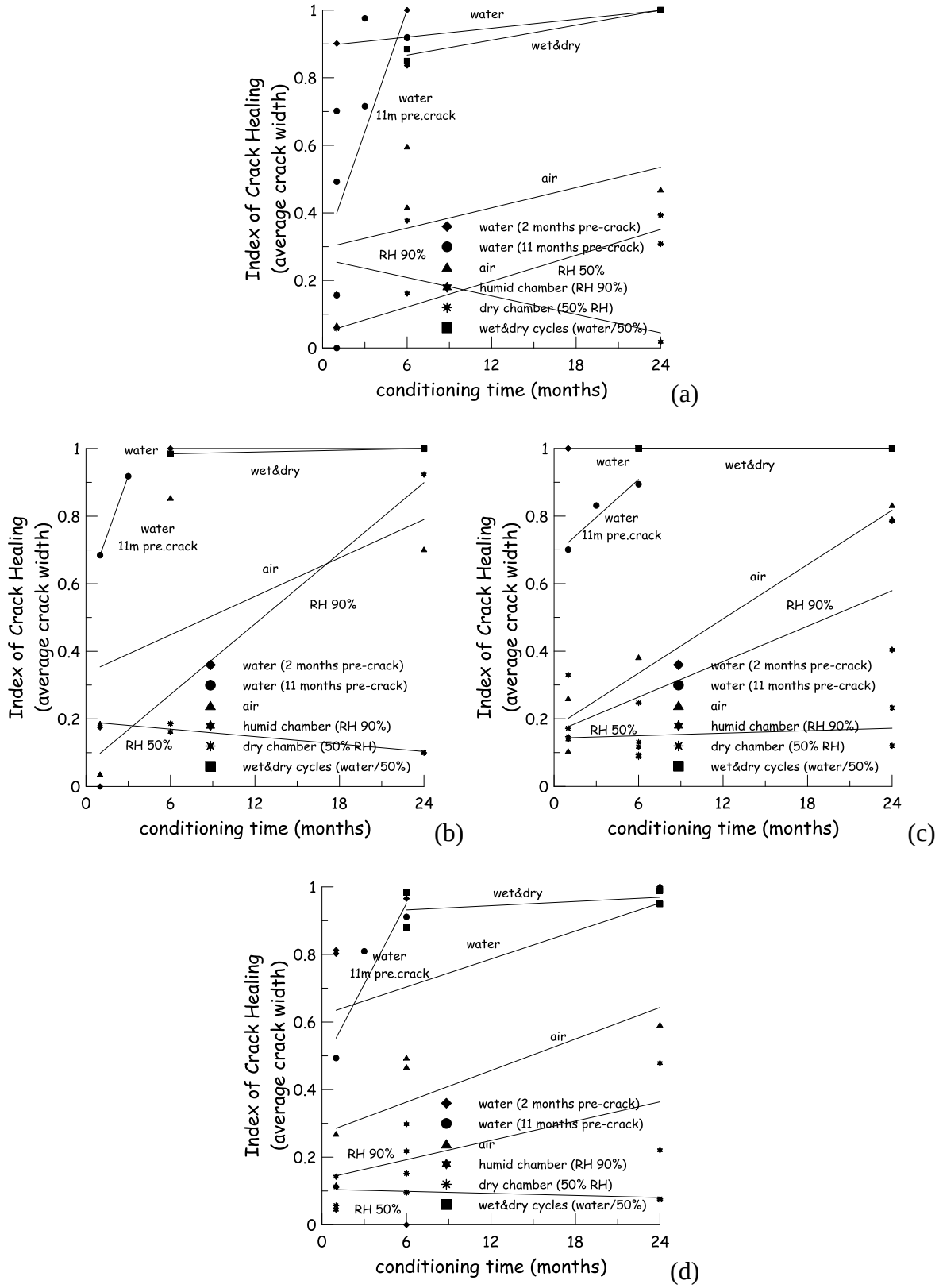


**Figure 13:** Index of Crack Healing, as per image processing (average crack width), vs. conditioning time for deflection softening (a) and hardening (b-d) specimens.

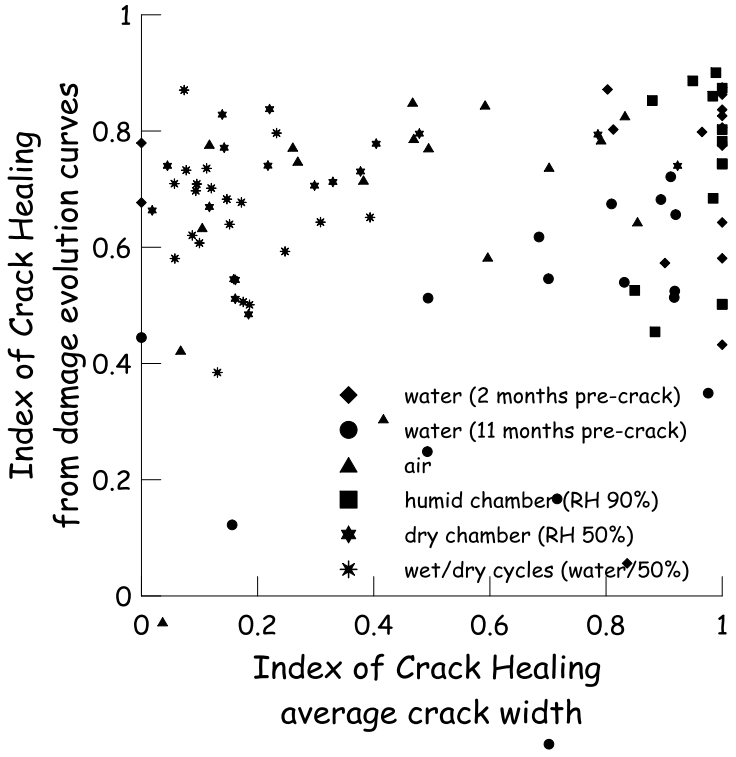


**Figure 14:** correlation between Index of Crack Healing from damage evolution curves vs. the Index of Crack Healing as per average crack width.

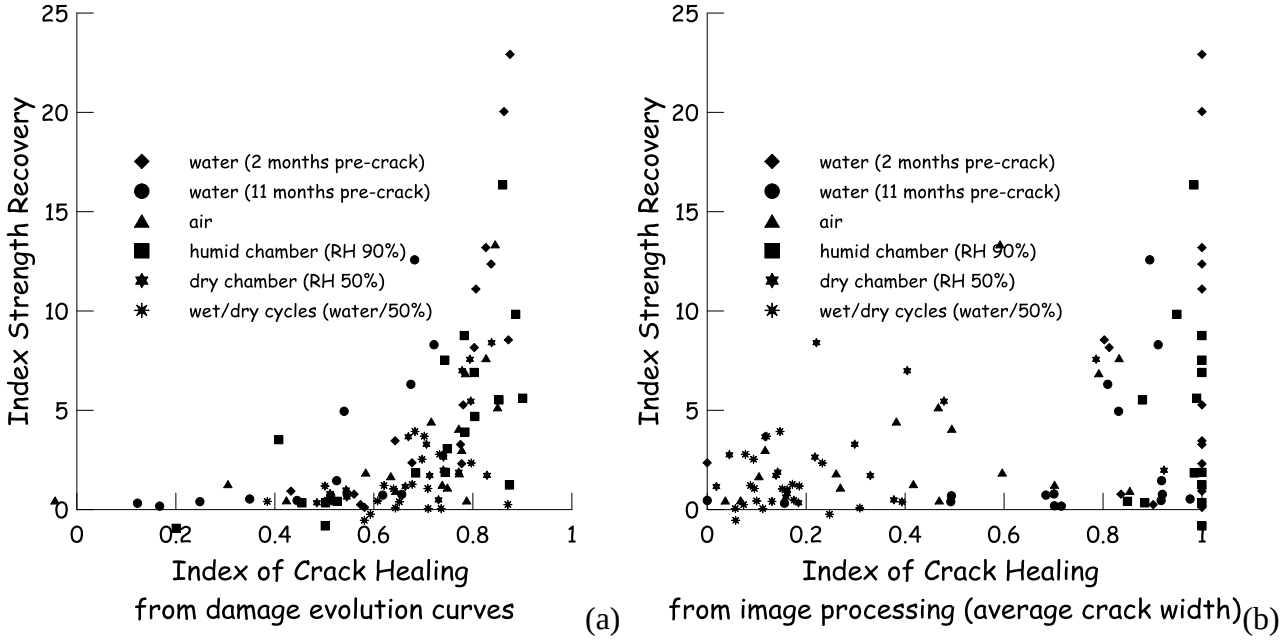


**Figure 15.** Correlation between Index of Strength Recovery and Index of Crack Healing as per damage evolution curves (a) and image processing (average crack width – b).

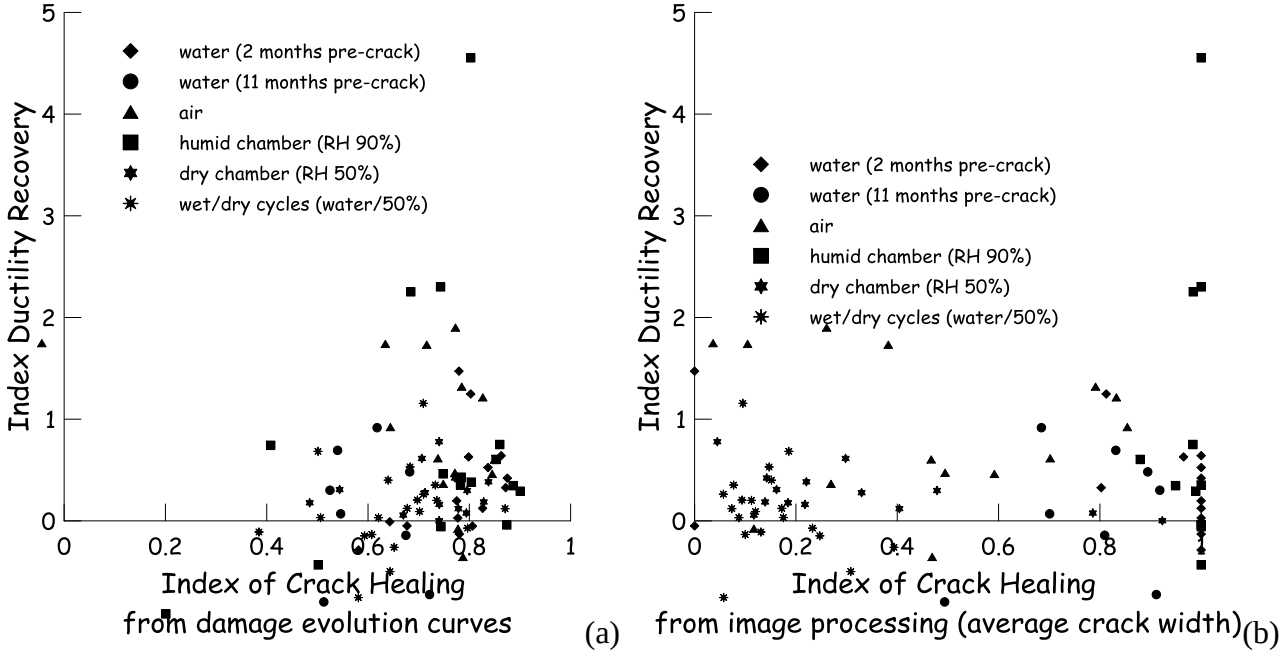


**Figure 16.** Correlation between Index of Ductility Recovery and Index of Crack Healing as per damage evolution curves (a) and image processing (average crack width – b).

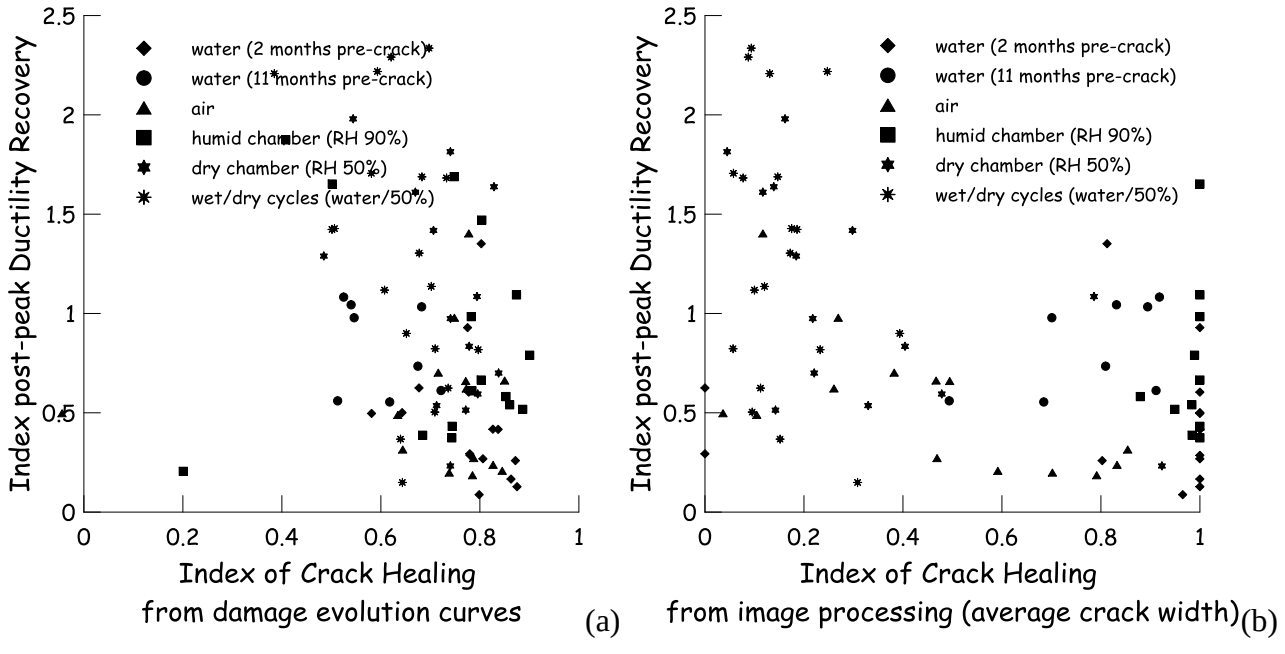


**Figure 17.** Correlation between Index of post-peak Ductility Recovery and Index of Crack Healing as per damage evolution curves (a) and image processing (average crack width – b).

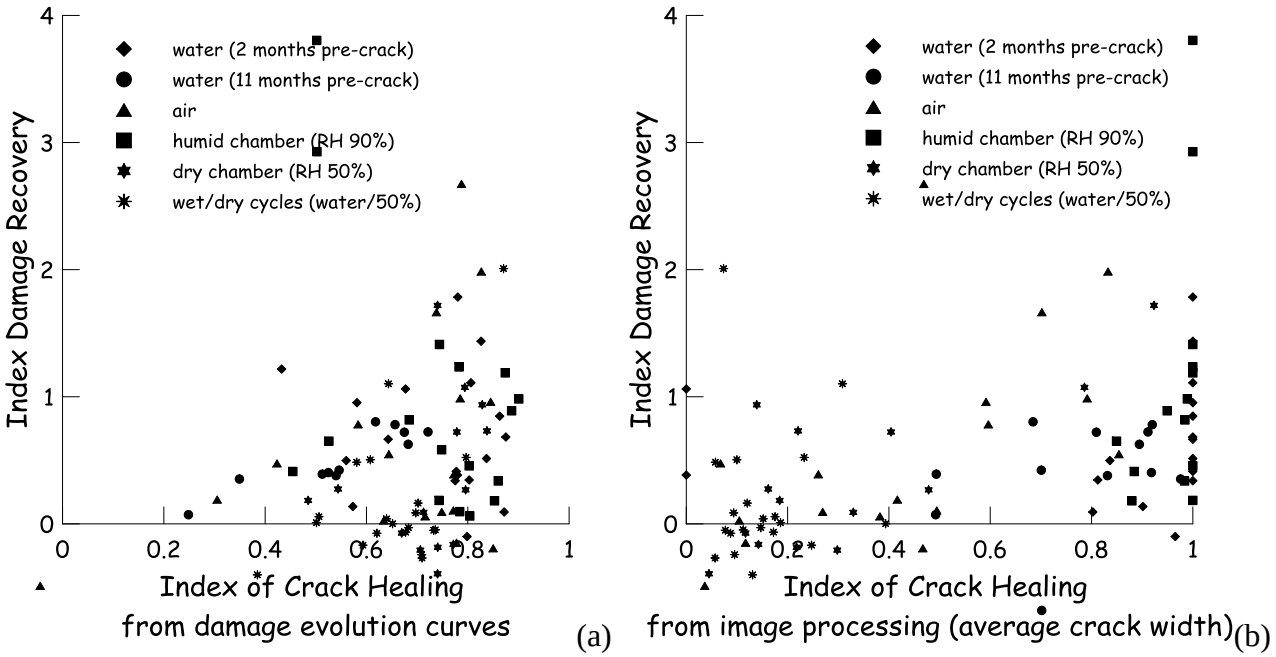


**Figure 18.** Correlation between Index of Damage Recovery and Index of Crack Healing as per damage evolution curves (a) and image processing (average crack width – b).

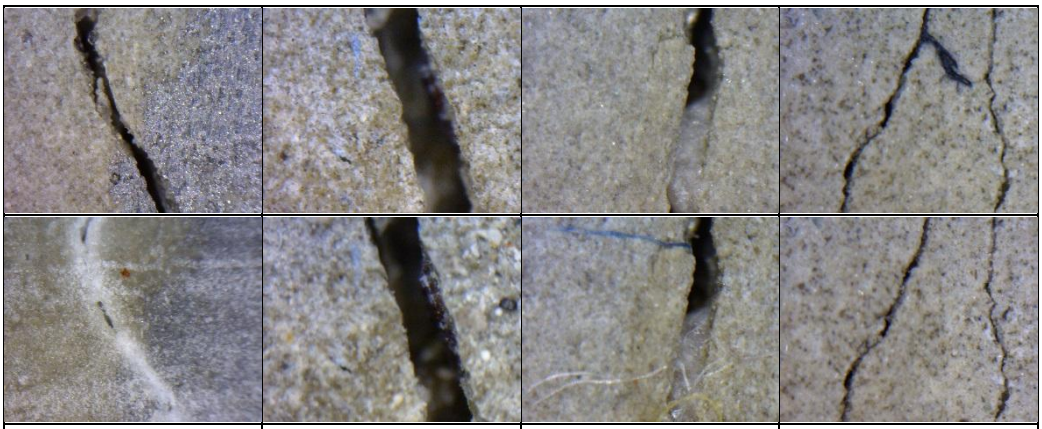

| 1 month in water | 1 month air | 1 month 90% RH | 1 month 50% RH |
|---|---|---|---|
| ISR 0.53 | (ISR 0.48 | ISR 0.64 | ISR 0.26 |
| IDaR 0.49 | IDaR 0.48 | IDaR 0.41 | IDaR 0.14 |
| ICHdamage 0.57 | ICHdamage 0.47 | ICH 0.55 | ICH 0.58 |
| ICHav.crack 0.9 | ICHav.cracn 0.07 | ICHAV. CRACK 0.16 | ICHAV. CRACK 0.06 |

**Figure 19a. –**Images of healed/healing cracks with related values of indices of recovery of mechanical properties and crack healing - deflection softening specimens – 1 month conditioning.

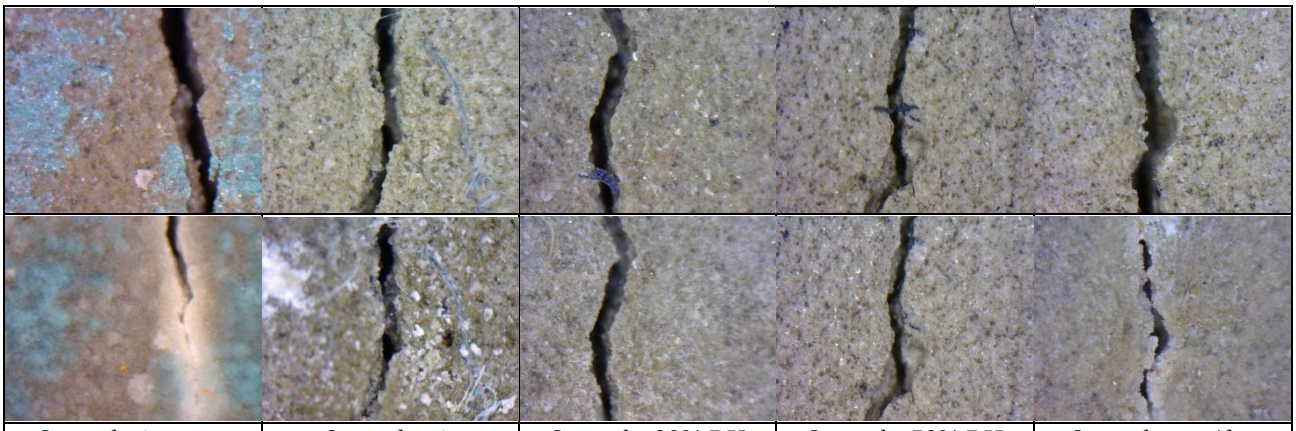

| 6 months in water | 6 months air | 6 months 90% RH | 6 months 50% RH | 6 months wet/dry |
|---|---|---|---|---|
| ISR 0.87 | ISR 0.78 | ISR 0.49 | ISR -0.23 | ISR 0.42 |
| IDaR 0.50 | IDaR 0.78 | IDaR 0.38 | IDaR -0.17 | IDaR 0.65 |
| ICHdamage 0.06 | ICHdamage 0.58 | ICHdamage 0.73 | ICHdamage 0.59 | ICHdamage 0.53 |
| ICHav.crack 0.9 | ICHav. crack 0.6 | ICHav. crack 0.38 | ICHav.crack 0.25 | ICHav.crack 0.85 |

**Figure 19b. –**Images of healed/healing cracks with related values of indices of recovery of mechanical properties and crack healing - deflection softening specimens – 6 months conditioning.

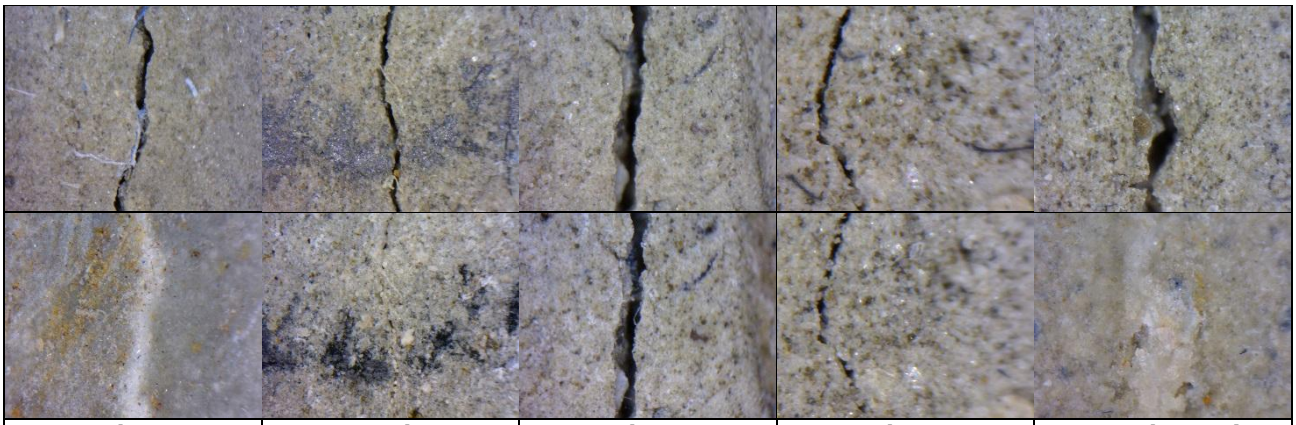

| 24 months in water | 24 months air | 24 months 90% RH | 24 months 50% RH | 24 months wet/dry |
|---|---|---|---|---|
| ISR 1.12 | ISR 0.47 | ISR 0.17 | ISR 0.09 | ISR 0.35 |
| IDaR 0.95 | IDaR 2.68 | IDaR 1.09 | IDaR 1.1 | IDaR 2.93 |
| ICHdamage 0.58 | ICHdamage 0.79 | ICHdamage 0.66 | ICHdamage 0.64 | ICHdamage 0.5 |
| ICHav. crack 1.0 | ICHav. crack 0.47 | ICHav. crack 0.02 | ICHav. crack 0.31 | ICHav. crack 1.0 |

**Figure 19c. –**Images of healed/healing cracks with related values of indices of recovery of mechanical properties and crack healing - deflection softening specimens – 24 months conditioning.

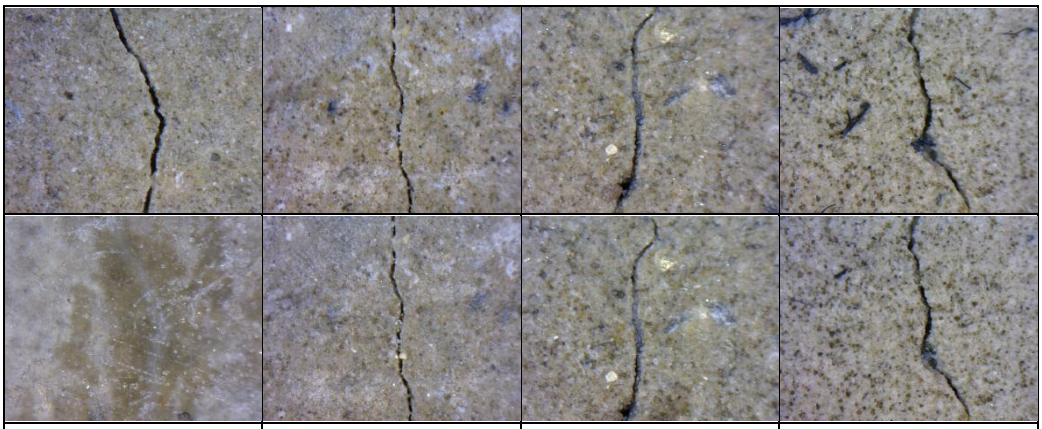

| 1 month in water | 1 month air | 1 month 90% RH | 1 month 50% RH |
|---|---|---|---|
| ISR 2.32 | ISR 1.69 | ISR 1.73 | ISR 3.94 |
| IDuR 0.03 | IDuR 1.74 | IDuR 0.19 | IDuR 0.53 |
| IDuRpost-peak 0.6 | IDuRpost-peak 0.49 | IDuRpost-peak 1.64 | IDuRpost-peak 1.69 |
| IDaR 0.41 | IDaR 0.03 | IDaR 0.94 | IDaR -0.03 |
| ICHdamage 0.78 | ICHdamage 0.63 | ICHdamage 0.83 | ICHdamage 0.68 |
| ICHav.crack 1.0 | ICHav. crack 0.1 | ICHav. crack 0.14 | ICHav. crack 0.15 |

**Figure 20a. –**Images of healed/healing cracks with related values of indices of recovery of mechanical properties and crack healing - deflection hardening specimens pre-cracked at 2 mm – 1 month conditioning.

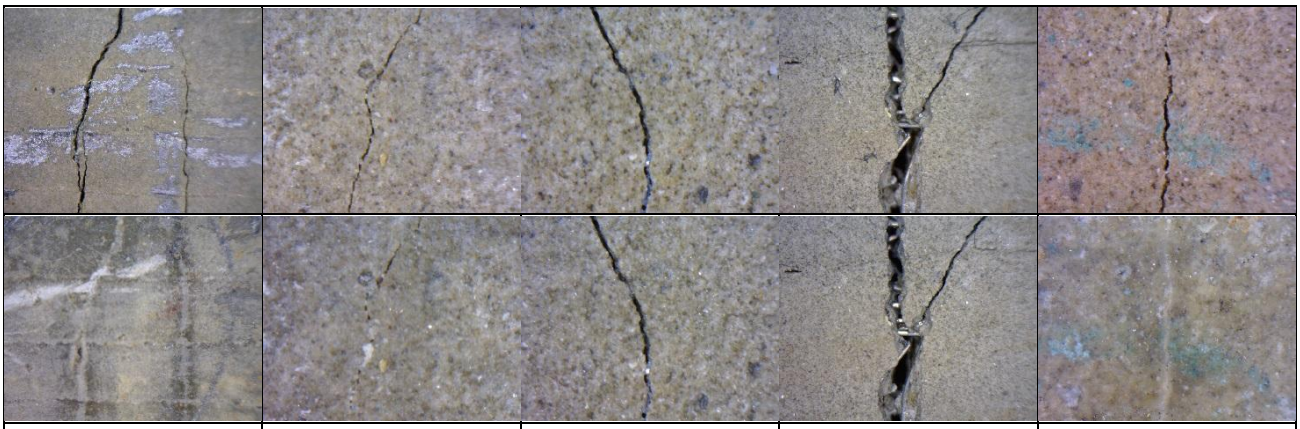

| 6 months in water | 6 months air | 6 months 90% RH | 6 months 50% RH | 6 months wet/dry |
|---|---|---|---|---|
| ISR 12.37 | ISR 4.44 | ISR 3.67 | ISR 0.42 | ISR 6.91 |
| IDuR 0.53 | IDuR 1.73 | IDuR 0.06 | IDuR -0.11 | IDuR 4.55 |
| IDuRpost-peak 0.42 | IDuRpost-peak 0.7 | IDuRpost-peak 1.61 | IDuRpost-peak2 2.21 | IDuRpost-peak 0.67 |
| IDaR 0.51 | IDaR 0.06 | IDaR -0.07 | IDaR -0.4 | IDaR 0.46 |
| ICHdamage 0.84 | ICHdamage 0.72 | ICHdamage 0.67 | ICHdamage 0.38 | ICHdamage 0.8 |
| ICHav.crack 1.0 | ICHav. crack 0.38 | ICHav.crack 0.12 | ICHav. crack 0.13 | ICHav.crack 1.0 |

**Figure 20b. –**Images of healed/healing cracks with related values of indices of recovery of mechanical properties and crack healing - deflection hardening specimens pre-cracked at 2 mm – 6 months conditioning.

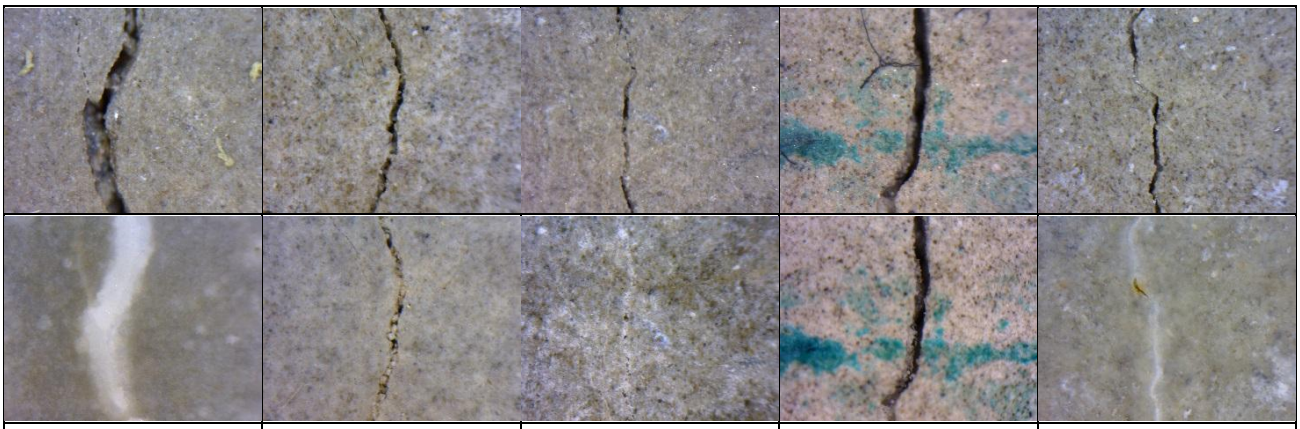

| | | | | |
|---|---|---|---|---|
| 24 months in water<br>ISR 11.11<br>IDuR -0.05<br>IDuRpost-peak 0.27<br>IDaR 1.11<br>ICHdamage 0.81<br>ICHav.crack 1.0 | 24 months air<br>ISR 7.63<br>IDuR 1.22<br>IDuRpost-.peak 0.24<br>IDaR 1.99<br>ICHdamage 0.83<br>ICHAV.<br>CRACKav.crack 0.83 | 24 months 90% RH<br>ISR 7.57<br>IDuR 0.08<br>IDuRpost-peak 1.09<br>IDaR 1.07<br>ICHdamage 0.79<br>ICHav. crack 0.79 | 24 months 50% RH<br>ISR 3.7<br>IDuR 0.09<br>IDuRpost-peak 1.14<br>IDaR 0.16<br>ICHdamage 0.7<br>ICHav. crack 0.12 | 24 months wet/dry<br>ISR 8.77<br>IDuR 0.35<br>IDuRpost-peak 0.98<br>IDaR 1.24<br>ICHdamage 0.78<br>ICHav. crack 1.0 |

**Figure 20c. –**Images of healed/healing cracks with related values of indices of recovery of mechanical properties and crack healing - deflection hardening specimens pre-cracked at 2 mm – 24 months conditioning.

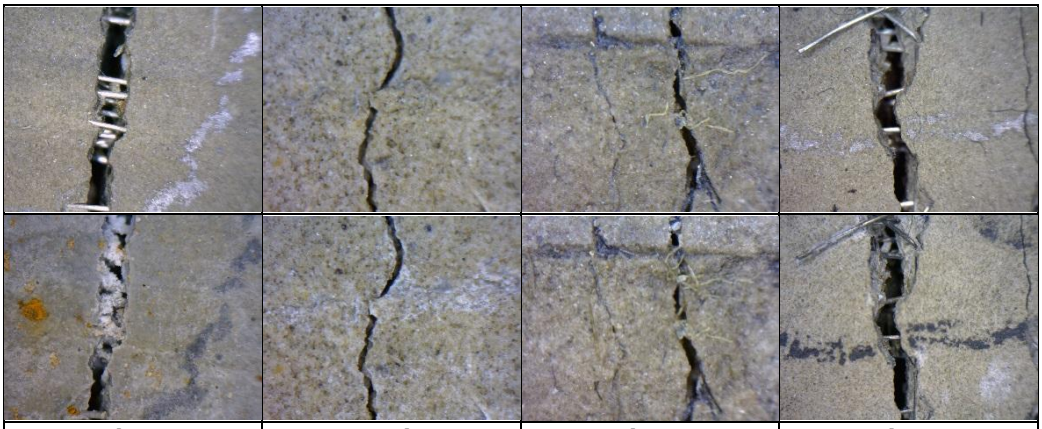

| | | | |
|---|---|---|---|
| 1 month in water<br>ISR 8.16<br>IDuR 1.25<br>IDuRpost-peak 1.35<br>IDaR 0.35<br>ICHdamage 0.8<br>ICHav. crack 0.81 | 1 month air<br>(ISR 1.12<br>IDuR 0.37<br>IDuRpost-peak 0.98<br>IDaR 0.1<br>ICHdamage 0.75<br>ICH av.crack 0.27 | 1 month 90% RH<br>ISR 2.76<br>IDuR 0.78<br>IDuRpost-peak 1.81<br>IDaR -0.39<br>ICHdamage 0.74<br>ICHav. crack 0.04 | 1 month 50% RH<br>ISR 0.06<br>IDuR 0.26<br>IDuRpost-peak 0.82<br>IDaR -0.27<br>ICHdamage 0.71<br>ICHav. crack 0.06 |

**Figure 21a. –**Images of healed/healing cracks with related values of indices of recovery of mechanical properties and crack healing - deflection hardening specimens pre-cracked at 0.5 mm after the peak – 1 month conditioning.

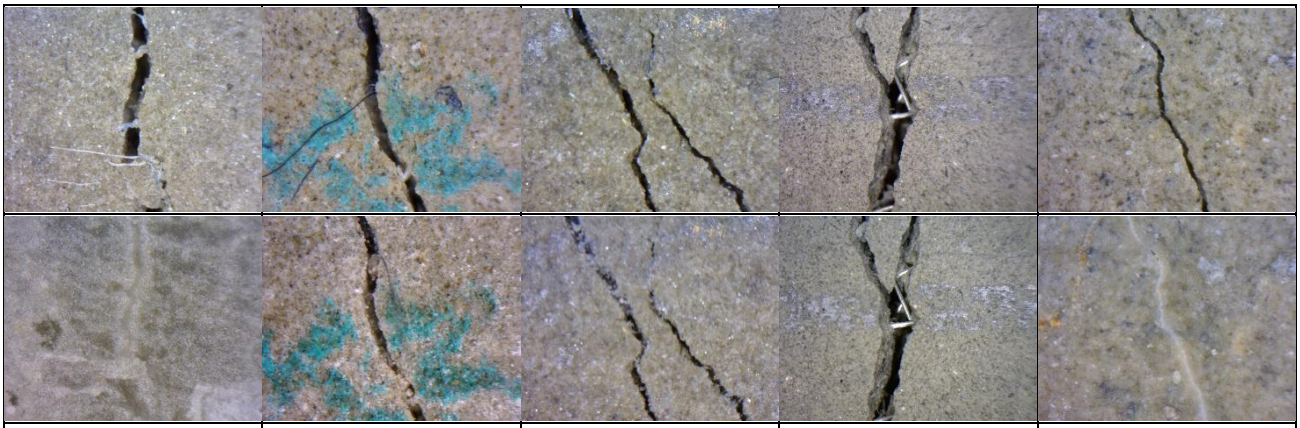

| 6 months in water | 6 months air | 6 months 90% RH | 6 months 50% RH | 6 months wet/dry |
|---|---|---|---|---|
| ISR 33.42 | ISR 5.16 | (ISR 3.3 | ISR 1.05 | ISR 16.35 |
| IDuR 0.63 | IDuR 0.61 | IDuR 0.62 | IDuR 0.4 | IDuR 0.75 |
| IDuRpost-peak 0.09 | IDuRpost-peak 0.66 | IDuRpost-peak 1.42 | IDuRpost-peak 0.37 | IDuRpost-peak 0.54 |
| IDaR -0.1 | IDaR -0.19 | IDaR -0.21 | IDaR 0.04 | IDaR 0.34 |
| ICHdamage 0.8 | ICHdamage 0.85 | ICHdamage 0.71 | ICHdamage 0.64 | ICHdamage 0.86 |
| ICHav. crack 0.97 | ICHav. crack 0.47 | ICHav. crack 0.1 | ICHav. crack 0.15 | ICHav. crack 0.98 |

**Figure 21b. –**Images of healed/healing cracks with related values of indices of recovery of mechanical properties and crack healing - deflection hardening specimens pre-cracked at 0.5 mm after the peak – 6 months conditioning.

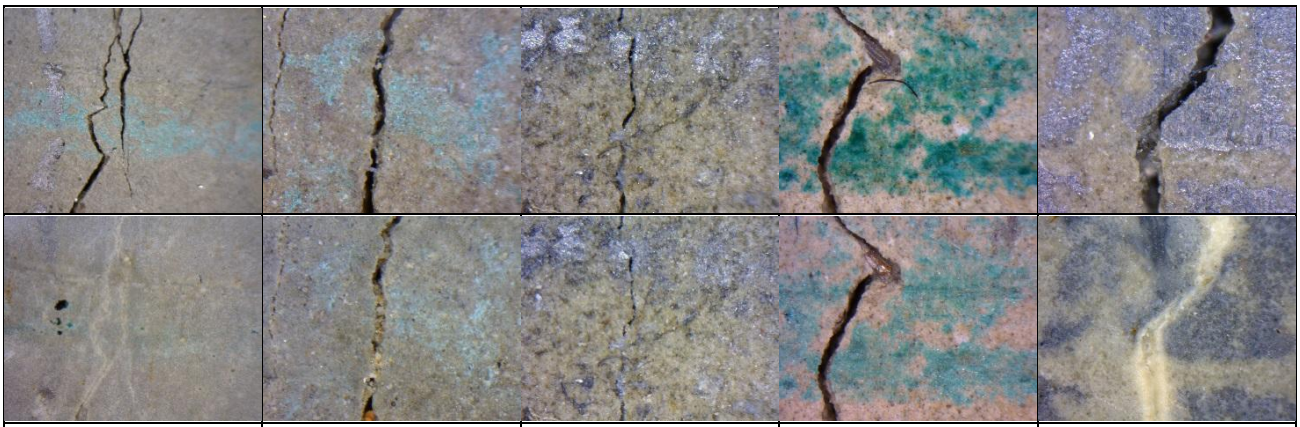

| 24 months in water | 24 months air | 24 months 90% RH | 24 months 50% RH | 24 months wet/dry |
|---|---|---|---|---|
| ISR 20.05 | ISR 13.36 | ISR 5.47 | ISR 0.26 | ISR 5.61 |
| IDuR 0.64 | IDuR 0.46 | IDuR 0.3 | IDuR 0.12 | IDuR 0.29 |
| IDuRpost-peak 0.17 | IDuRpost-peak 0.21 | IDuRpost-peak 0.6 | IDuRpost-peak 4.22 | IDuRpost-peak 0.79 |
| IDaR 0.85 | IDaR 0.96 | IDaR 0.27 | IDaR 2.01 | IDaR 0.98 |
| ICHdamage 0.86 | ICHdamage 0.85 | ICHdamage 0.8 | ICHdamage 0.87 | ICHdamage 0.9 |
| ICHav. crack 1.0 | ICHav. crack 0.59 | ICHav. crack 0.48 | ICHav. crack 0.07 | ICHav. crack 0.97 |

**Figure 21c. –**Images of healed/healing cracks with related values of indices of recovery of mechanical properties and crack healing - deflection hardening specimens pre-cracked at 0.5 mm after the peak – 24 months conditioning.